genesis 49:488–513 (2011)

REVIEW

Reconstructing Embryonic Development

Khaled Khairy and Philipp J. Keller*

Janelia Farm Research Campus, Howard Hughes Medical Institute, 19700 Helix Drive, Ashburn, Virginia

Received 12 October 2010; Revised 22 November 2010; Accepted 24 November 2010

Summary: Novel approaches to bio-imaging and automated computational image processing allow the design of truly quantitative studies in developmental biology. Cell behavior, cell fate decisions, cell interactions during tissue morphogenesis, and gene expression dynamics can be analyzed in vivo for entire complex organisms and throughout embryonic development. We review state-of-the-art technology for live imaging, focusing on fluorescence light microscopy techniques for system-level investigations of animal development, and discuss computational approaches to image segmentation, cell tracking, automated data annotation, and biophysical modeling. We argue that the substantial increase in data complexity and size requires sophisticated new strategies to data analysis to exploit the enormous potential of these new resources. genesis 49:488–513, 2011. © 2010 Wiley-Liss, Inc.

Key words: quantitative developmental biology; light microscopy; image processing; biophysical modeling; *in toto* reconstruction

INTRODUCTION

Recent years have seen a number of technological advances, which likely will open up entirely new avenues to studying the development of complex multicellular organisms. Breakthroughs in light microscopy technology are accompanied by new computational tools for automated image processing and data analysis. At the same time processing power of consumer-level computers increases at a fast pace and high-performance computational hardware is available at very low cost. Fast imaging platforms are interfaced with powerful computational infrastructures for routine investigations in the life sciences.

Since system-wide experimental investigations of development are now accessible in vertebrates and higher invertebrates, the spectrum of new possibilities is extensive. The development of tissues and entire organs can be studied in live animals at single-cell resolution. Cell migratory tracks, cell division patterns, and lineage trees can be extracted and tested against biophysical models of cell behavior and cell mechanics. Large-scale comparative analyses provide information on the variability of developmental building plans and allow the quantitative assessment of mutant defects. Such morphogenetic reconstructions can be complemented by comprehensive analyses of gene expression patterns, yielding high-resolution atlases for different developmental stages.

An obvious next step is the extension to a complete in silico database with information on gene expression, cell lineages, and a morphogenetic description of cellular dynamics (Paluch and Heisenberg, 2009) for all cells throughout the entire period of development (Megason and Fraser, 2007). A long-term goal of these efforts is the system-level understanding of developing organisms. Combining a comprehensive set of morphological, genetic, and functional in vivo data with sophisticated computational processing strategies may ultimately allow the construction of a descriptive model of embryogenesis. A quantitative assessment of these complex data may allow the extraction of a fundamental set of mechanistic rules in a normalized morphogenetic scaffold and thus pave the way for a developmental computer model with truly predictive power.

Challenges in Imaging-Based Studies of Embryonic Development

System-wide quantitative studies of development are becoming increasingly popular (Mavrakis *et al.*, 2010).

*Correspondence to: Dr. Philipp J. Keller, Janelia Farm Research Campus, Howard Hughes Medical Institute, 19700 Helix Drive, Ashburn, VA 20147, USA.
E-mail: kellerp@janelia.hhmi.org
Published online 7 December 2010 in
Wiley Online Library (wileyonlinelibrary.com).
DOI: 10.1002/dvg.20698

The first critical step in the experimental workflow is data acquisition, which is most frequently implemented using fluorescence light microscopy assays. Fluorescence light microscopy provides specificity, good spatio-temporal resolution and is well-suited for in vivo studies of sufficiently transparent specimens. This set of attributes is complemented by other imaging modalities, such as microscopic magnetic resonance imaging (μMRI), which trades off specificity and resolution, but achieves outstanding coverage in large opaque specimens (Jacobs et al., 2003). The excellent penetration provided by μMRI is critical e.g. in studies of amphibian (Papan et al., 2007) and avian (Ruffins et al., 2007) embryogenesis.

In this review, we will primarily focus on fluorescence light microscopy assays, which are particularly well established in the life sciences and have been instrumental in dissecting developmental mechanisms in various biological model systems. There are many experimental challenges in the comprehensive study of cell behavior in entire intact organisms. Desirable—and often critical—properties of the microscope are a high imaging speed, high signal-to-noise ratio, efficient, and comprehensive coverage of large embryos in their entirety, good spatial resolution, physiological imaging at low levels of photo-toxicity and low levels of photobleaching. Live imaging of large cell populations or even entire embryos at single-cell resolution requires fast data acquisition, if cell identities are to be followed unambiguously over time. Precise mapping requires excellent computational segmentation efficiency in combination with sampling speeds that yield cell movement distances of less than half a cell diameter within the sampling interval. In zebrafish and *Drosophila* embryos, this typically corresponds to sampling intervals of about 60 s and 30 s, respectively. High signal-to-noise ratio and spatial resolution are critical to achieve good detection efficiencies in an automated computational analysis of the microscopy data. This is particularly important in fluorescence microscopy, as image quality degrades with increasing imaging depth into the specimen and labeling/expression efficiency of fluorescent markers typically varies from cell to cell. For long-term observations, e.g., when studying organ development or reverse-engineering cell fate decisions, it is furthermore critical to employ assays that ensure minimal photo-damage in the specimen. Similarly, the consumption of fluorophores in the excitation process requires optimal use of the limited photon budget provided by the fluorescent markers in the specimen.

Studying Development With Confocal and Two-Photon Laser-Scanning Microscopy

In the last decade, conventional and confocal fluorescence microscopy were the most frequently used techniques for quantitative imaging of development (Pawley, 2006), followed by multiphoton techniques (Denk *et al*., 1990; Diaspro *et al*., 2005; Helmchen and Denk, 2005). In addition, a number of complementary methods, such as Optical Projection Tomography (Sharpe *et al*., 2002) and Optical Coherence Tomography (Huang *et al*., 1991), were developed and applied to a broad spectrum of biological questions and model organisms, including live imaging of early mouse development (Larin *et al*., 2009).

The most common implementations of confocal and two-photon microscopy are based on two-dimensional laser scanning. A laser beam is focused into the specimen and fluorescence light emitted by fluorophores in the respective focal volume is collected by using the same objective. Subsequently, the laser focus is moved to the next location. In this manner, image information is obtained pixel per pixel until an entire thin volume section has been covered and represented in a two-dimensional image. The pixel dwell time (the resting time of the laser on each spot) is typically in the order of 1–10 μs, and thus it takes about 1–10 s to record a typical one-megapixel-sized image. While conventional confocal fluorescence microscopy relies on one-photon excitation, i.e., fluorophore excitation by absorption of a single photon of the illuminating laser beam, two-photon microscopy uses light of a longer wavelength, which enables excitation only upon near-simultaneous absorption of two photons by the same fluorophore. Two-photon microscopy provides intrinsic optical sectioning, as the high photon densities required for efficient excitation occur only in the small focal volume. In contrast, one-photon excitation-based confocal microscopes require the use of a small pinhole in the detection system to block fluorescence originating from out-of-focus regions. An increase in imaging speed is achieved in spinning disk confocal microscopes (Graf *et al*., 2005) and in line-scanning implementations, which collect information for multiple pixels simultaneously. The increase in imaging speed comes at the expense of image quality, since the parallelized illumination/detection scheme leads to signal cross-talk between different volume elements.

Traditional experimental approaches based on confocal and two-photon fluorescence microscopy are well established and are often used for live observation of subpopulations of cells in the developing embryo. Imaging is typically performed either over short periods of time with high temporal sampling or over long periods of time with intermediate temporal sampling.

Confocal light microscopy has enabled detailed studies of the embryogenesis of *Caenorhabditis elegans*, including the automated reconstruction of comprehensive cell lineage trees (Bao *et al*., 2006; Murray *et al*., 2006) and the automated analysis of gene expression patterns (Liu *et al*., 2009b; Long *et al*., 2009; Murray *et al*., 2008; Murray *et al*., 2006; Peng *et al*., 2008). Confocal time-lapse imaging of morphogenesis has also

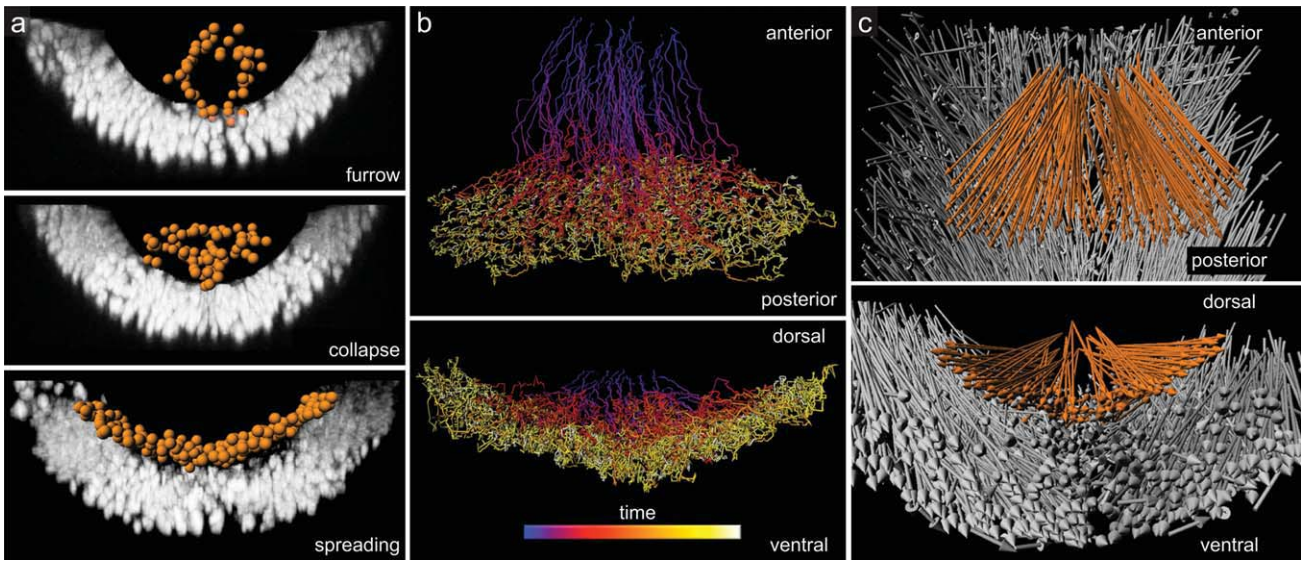

FIG. 1. Imaging and reconstructing *Drosophila* gastrulation with two-photon microscopy. (**a**) Segmentation of mesoderm nuclei (orange spheres) in histone-GFP expressing embryos by the use of Imaris software. Furrow formation, furrow collapse as a result of an epithelial-to-mesenchymal transition, and spreading of the mesoderm to form a monolayer are illustrated from top to bottom, respectively. (**b/c**) Tracking cell positions in three dimensions over time. Shown are dorsal (b, upper panel) and posterior (b, lower panel) views of mesoderm tracks (blue and yellow indicate early and late time points, respectively) and dorsal (c, upper panel) and posterior (c, lower panel) views of mesoderm (orange), and ectoderm (gray) net displacement vectors. Scale bars, 20 μm. Credits: Panels (a–c) were reprinted from *Science*, vol. 322, McMahon *et al*., "Dynamic Analyses of *Drosophila* Gastrulation Provide Insights into Collective Cell Migration", 1546-1550, Copyright (2008), with permission from AAAS.

been established in ascidians (Rhee *et al*., 2005) and annelids and recently allowed constructing high-resolution gene expression maps for the developing *Platynereis dumerilii brain* (*Tomer et al*., 2010). In less transparent species, such as *Drosophila melanogaster*, two-photon microscopy typically provides superior accessibility of dynamic processes deep inside the embryo (Fowlkes *et al*., 2008; Parton *et al*., 2010), as has been demonstrated in the analysis of germ layer formation during gastrulation (McMahon *et al*., 2008; Supatto *et al*., 2009) (see Fig. 1). By introducing quantitative modeling and image registration, two-photon microscopy-based assays enabled the construction of an extensive gene-expression atlas for several developmental stages in the early fly embryo (Fowlkes *et al*., 2008; Luengo Hendriks *et al*., 2007; Luengo Hendriks *et al*., 2006) (see Figure 2). Dynamic events in superficial structures, such as the remodeling of epidermal tissue during dorsal closure (Solon *et al*., 2009), are also readily accessible by confocal microscopy (Mavrakis *et al*., 2008), and, if live imaging is not a critical requirement, confocal microscopy can be combined with chemical clearing protocols (Spalteholz, 1914) to enhance depth penetration in systems-level studies.

While early *Drosophila* embryos are generally difficult to image due to strong light scattering/absorption and auto-fluorescence of yolk granules and the vitelline membrane (Mavrakis *et al*., 2008), the highly transparent embryos of e.g. the fish species *Danio rerio* and *Oryzias latipes* lend themselves very well to fluorescence microscopy-based imaging assays (Megason and Fraser, 2003, 2007; Wittbrodt *et al*., 2002). Numerous quantitative analyses of their development have been performed, including studies of axis elongation (Gong *et al*., 2004), cell sorting during germ layer formation (Krieg *et al*., 2008), convergence and extension (Yin *et al*., 2009), early forebrain development and fate mapping (England and Adams, 2007; England *et al*., 2006), optic vesicle formation (Rembold *et al*., 2006), morphogenesis of neural crest (Ezin *et al*., 2009) and late brain development (Hirose *et al*., 2004; Koster and Fraser, 2004). Exceptionally fast events can be captured by optimizing imaging speeds with slit-scanning confocal microscopy, e.g., for analyzing the developmental dynamics of the beating embryonic heart (Liebling *et al*., 2006).

In addition to confocal and two-photon fluorescence microscopy, harmonic generation microscopy has been used for the in vivo study of zebrafish embryos, combining second- and third-harmonic generation microscopy for label-free imaging (Chen *et al*., 2006; Chu *et al*., 2003; Hsieh *et al*., 2008; Sun *et al*., 2004). A modification of this technique allowed cell lineaging for the first three hours of early zebrafish embryogenesis (Olivier *et al*., 2010).

Studying avian and mammalian embryogenesis is particularly challenging, as it requires not only elaborate microscopy, but also sophisticated in vivo assays or in vitro embryo culture. These assays are complemented by powerful genetic tools, e.g., for functional genomics

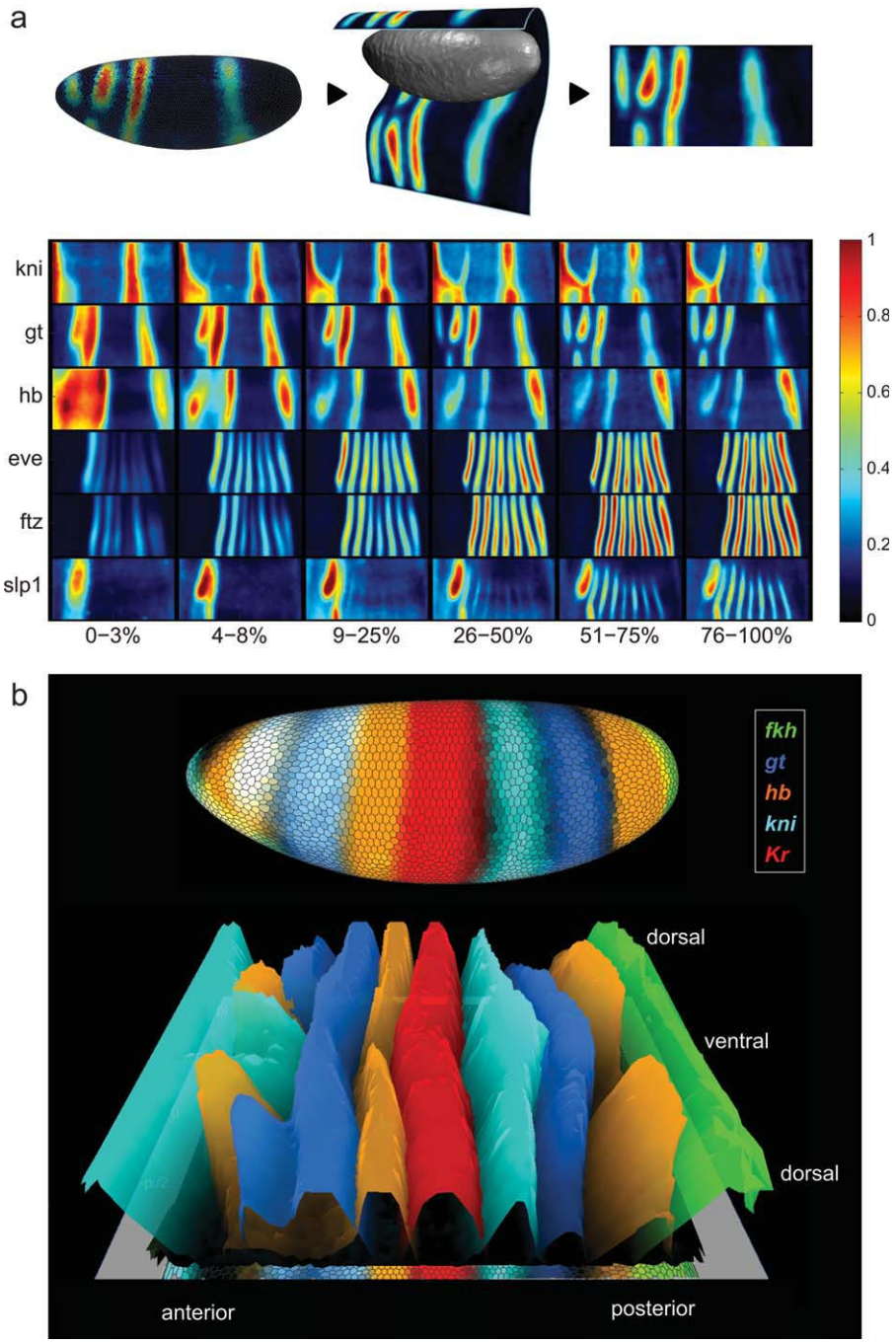

FIG. 2. Quantitative mapping of gene expression patterns in the *Drosophila* blastoderm. (**a**) Examples of average temporal patterns of mRNA expression recorded in the *Drosophila* VirtualEmbryo for several gap (kni, gt, hb) and pair-rule (eve, ftz, slp1) genes. Temporal cohorts, staged by percent membrane invagination, are arranged from left to right with each row corresponding to a different gene. Each rectangle shows a lateral view of the blastoderm in a half-cylindrical projection with the dorsal midline at top, the ventral midline at the bottom, and anterior to the left. (**b**) PointCloudXplore allows visualization of quantitative three-dimensional expression data. Expression of the gap genes fkh, gt, hb, kni, and Kr is shown for the stage 5: 4–8% cohort. The upper panel shows a three-dimensional model of the blastoderm surface (anterior left, dorsal down) with each nucleus colored according to the expression level of the five genes. The lower panel shows a cylindrical projection of the entire blastoderm (anterior left, ventral center, dorsal upper, and lower edges). The heights of each surface plot indicate the average expression level of the gene recorded at that point on the VirtualEmbryo, making readily visible the quantitative changes in expression of these gap genes along both the A-P and D-V axes. A comprehensive database of gene expression patterns and the PointCloudXplore software are available at http://bdtnp.lbl.gov/Fly-Net/bioimaging.jsp. Credits: Panels (a/b) were reprinted from *Cell*, vol. 133, Fowlkes *et al*., "A Quantitative Spatiotemporal Atlas of Gene Expression in the *Drosophila* Blastoderm", 364-674, Copyright (2008), with permission from Elsevier.

and in vivo cell tracking in mice (Hadjantonakis et al., 2003; Hadjantonakis and Papaioannou, 2004; Nowotschin and Hadjantonakis, 2009a,b). Comprehensive protocols have been devised for the in ovo imaging of chick somitogenesis (Kulesa et al., 2010; Kulesa and Fraser, 2002) and live mouse imaging in embryo culture (Nowotschin et al. 2010; Udan and Dickinson, 2010). The quite remarkable progress in these fields and the development of new tools for live imaging of early mouse development open up an exciting perspective for quantitative studies of development in higher vertebrates (Chuai et al., 2009; Chuai and Weijer, 2009; Nowotschin *et al.*, 2009; Nowotschin and Hadjantonakis, 2010).

Confocal fluorescence microscopes are faster than two-photon microscopes and yield data at a better signal-to-noise ratio, whereas two-photon excitation typically provides improved penetration depth in live tissues due to the wavelength-dependency of the magnitude of light scattering and light absorption (McMahon *et al.*, 2008; Supatto *et al.*, 2009). Owing to extensive research efforts and iterative optimization in numerous commercial designs, today's confocal and two-photon fluorescence microscopes are both powerful and straightforward to apply. However, there are also fundamental limitations that make certain types of experimental investigations impossible. In both cases the point-scanning approach leads to technical limitations in imaging speed, efficient use of the fluorescent markers, or both, which preclude the system-wide study of cell behavior at the spatio-temporal resolution required for comprehensive cell tracking in entire animals throughout development. Moreover, at relatively high imaging speeds the maximum time window of observation in the confocal fluorescence microscope is typically limited to a few hours at maximum due to the effects of photo-bleaching and -toxicity.

Studying Development With Light Sheet-Based Microscopy

The fundamental limitations in imaging speed, signal-to-noise ratio and photon-efficiency of point-scanning microscopy modalities, such as confocal and two-photon fluorescence microscopes, were overcome with the advent of light sheet-based fluorescence microscopy. Initially developed for macroscopic imaging (Siedentopf and Zsigmondy, 1903; Voie *et al.*, 1993), the method was developed further for fluorescence microscopy of biological specimens (Fuchs *et al.*, 2002; Huisken *et al.*, 2004).

The basic idea behind light sheet microscopy is to employ two separate optical subsystems oriented perpendicular to each other (Stelzer and Lindek, 1994), which are used for light sheet illumination and fluorescence detection, respectively (Fig. 3a). The first subsystem creates a laser light sheet either by using a suitable optical element, such as a cylindrical lens (Huisken *et al.*, 2004), or by using laser scanners (Keller *et al.*, 2008b) (Fig. 3b). The second optical subsystem detects the fluorescence emitted by fluorophores in the illuminated plane via a conventional camera-based wide-field detection arrangement. While nonscanning light sheet microscopy is optically and electronically easier to implement, the scanning approach provides increased flexibility and control over the illumination profile, which is critical e.g. for contrast-enhancing structured illumination (DSLM-SI, Figure 3c) (Keller *et al.*, 2010) and fast three-dimensional imaging of stationary samples. The intrinsic incoherence of the scanned light sheet implementation furthermore provides improved homogeneity of sample illumination and thereby increases image quality (Rohrbach, 2009).

Light sheet microscopy provides intrinsic optical sectioning. Imaging speed and signal-to-noise ratio are exceptionally high due to the parallelized detection scheme. At the same time, photo-damage in the specimen is substantially reduced, since only the thin volume in the focus of the detection subsystem is illuminated to acquire an image. This combination of advantages is critical for live imaging applications and allows high-speed imaging of cell behavior in entire vertebrate and higher invertebrate embryos at subcellular resolution (Keller *et al.*, 2010; Keller *et al.*, 2008b).

Light sheet-based microscopes typically employ water-dipping lenses with long working distance as well as vertical sample mounting, which provide intrinsic capability of multiview imaging. This imaging mode refers to the acquisition of a series of data sets of the same volume along multiple angles (Fig. 3a). The advantages are two-fold: In large specimens that are not visible in their entirety from a single view due to their size or other factors limiting optical penetration depth, multiview imaging allows structural complementation and reconstitution of a single data set representing the entire specimen (Huisken *et al.*, 2004; Keller *et al.*, 2010; Keller *et al.*, 2008b; Preibisch *et al.*, 2010). In addition, multiview imaging can be used to overcome the anisotropy of the point spread function resulting from the use of a single detection lens arrangement employed in almost all light microscopy implementations. Whereas the axial resolution is typically inferior to the lateral resolution in single-view imaging—usually by approximately one order of magnitude—a data set with isotropic resolution can be reconstructed in multiview imaging (Keller *et al.*, 2006; Swoger *et al.*, 2007; Verveer *et al.*, 2007). More detailed technical descriptions of light sheet microscopy and comparisons to conventional confocal and two-photon microscopy with respect to the parameters discussed above are provided elsewhere (Huisken and Stainier, 2009; Keller and Stelzer, 2008, 2010).

Light sheet-based microscopy is highly amenable to integration with other optical techniques. Examples of

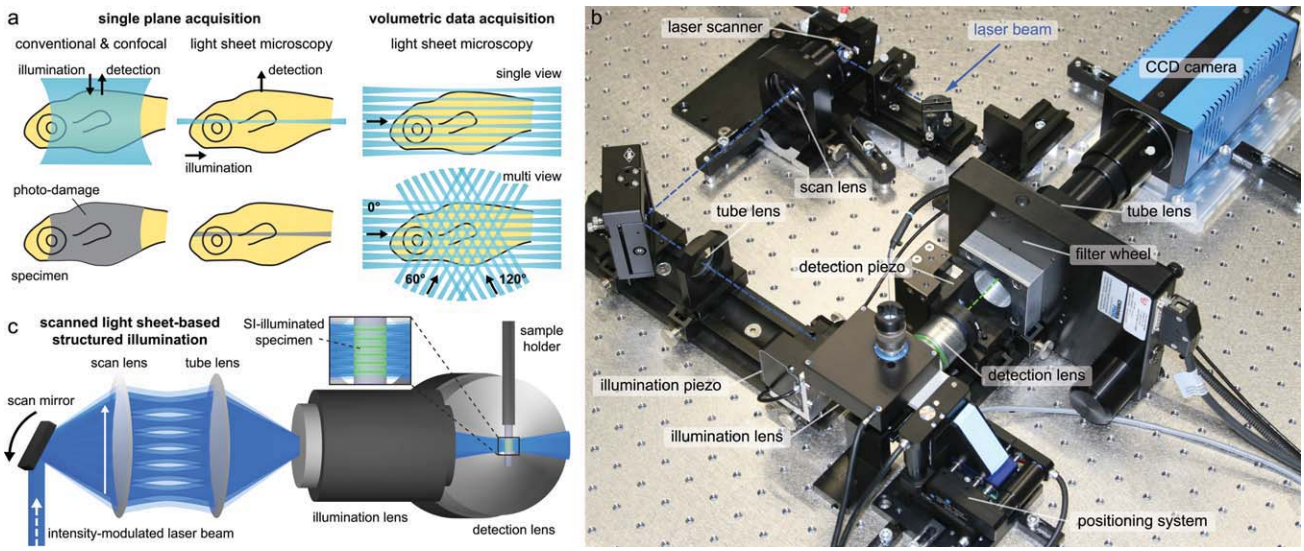

FIG. 3. Light sheet-based microscopy. (**a**) Left: Comparison of sample illumination and fluorescence detection in conventional/confocal microscopy and in light sheet-based microscopy (LSFM). A major part of the specimen is illuminated in confocal microscopy, although fluorescence from only a single plane in the specimen is detected. By contrast, no photo-damage is inflicted outside the in-focus plane of the detection system in the light sheet-based microscope. Right: Three-dimensional imaging in light sheet-based microscopy is performed by moving the specimen through the light sheet in small steps and recording a two-dimensional image at each step. In DSLM, three-dimensional imaging can alternatively be performed by moving the light sheet through the specimen and by displacing the detection lens accordingly. In multiview imaging, the same volume inside the specimen or even the entire specimen is recorded along several angles. The resulting multiview information can be combined into a single image stack by data post-processing using a fusion algorithm. (**b**) Photograph of the central part of the DSLM-SI imaging platform with a single CCD camera for fluorescence detection. The figure shows the DSLM subsystems for illumination (blue dashed line) and detection (green dashed line). (**c**) Light sheet-based structured illumination with digitally adjustable frequency: Side view of the central components of a digital scanned laser light-sheet fluorescence microscope. The illumination lens illuminates a thin volume by rapidly scanning a micrometer-sized laser beam through the specimen. Fluorescence is detected at a right angle to the illuminated plane by the detection lens. The intensity of the laser beam is modulated in synchrony with the scanning process to create the structured illumination light patterns. Credits: Panel (a) was reprinted from *Current Opinion in Neurobiology*, vol. 18, Keller and Stelzer, "Quantitative *in vivo* imaging of entire embryos with Digital Scanned Laser Light Sheet Fluorescence Microscopy", 624-632, Copyright (2008), with permission from Elsevier. Panels (b/c) were reprinted from *Nature Methods*, vol. 7 no. 8, Keller *et al*., "Fast, high-contrast imaging of animal development with scanned light sheet-based structured-illumination microscopy", 637-642, Copyright (2010), with permission from Macmillan Publishers Ltd.

such extensions are the introduction of laser ablation for precise three-dimensional sample manipulation (Engelbrecht *et al*., 2007) and the use of two-photon excitation to achieve a further increase of penetration depth, albeit at the expense of signal-to-noise ratio and flexibility in multi-color imaging (Palero *et al*., 2010).

The exceptionally low levels of photobleaching and phototoxicity in light sheet-based microscopy not only have a quantitative impact on the recordings, but also enable entirely new experimental observations. Examples are the imaging of fast cytoskeletal dynamics in three dimensions over long periods of time (Keller *et al*., 2008a; Keller *et al*., 2007) or the observation of zebrafish development over three days at high spatio-temporal resolution (Keller *et al*., 2010). The advantages arising from low illumination energy requirements are further complemented by new assays for physiological three-dimensional sample preparation, using low-concentration agarose cylinders (Huisken *et al*., 2004; Keller *et al*., 2008b) or soft gels such as collagen I or reconstituted basement membrane (Pampaloni *et al*., 2007), conventional coverslip-based experimental preparations.

While scanning (DSLM) (Keller *et al*., 2010; Keller *et al*., 2008b; Keller and Stelzer, 2008, 2010; Mertz and Kim, 2010) and nonscanning (SPIM, mSPIM, OPFOS, TLSM, OCPI, Ultramicroscopy) (Buytaert and Dirckx, 2007; Dodt *et al*., 2007; Fuchs *et al*., 2002; Holekamp *et al*., 2008; Huisken and Stainier, 2007, 2009; Huisken *et al*., 2004; Keller *et al*., 2006, 2007; Turaga and Holy, 2008) implementations of light sheet-based microscopy have shown exceptional capabilities in a wide spectrum of applications in the life sciences, their intrinsic advantages are invaluable in the comprehensive study of cell behavior in complex developing organisms. Light sheet microscopy has been applied to analyze cellular dynamics in entire wild-type and mutant zebrafish embryos over 24 hours (Keller *et al*., 2008b) (Figures 4 and 5, http://www.digital-embryo.org/fish.html), to follow zebrafish brain development with cellular resolution over 3 days (Keller *et al*., 2010) and for high-speed imaging of the embryonic heart to study atrioventricular valve morphogenesis and function (Scherz *et al*., 2008). Combining scanned light sheet microscopy with structured illumination patterns (DSLM-SI, Figure 3c) provides high

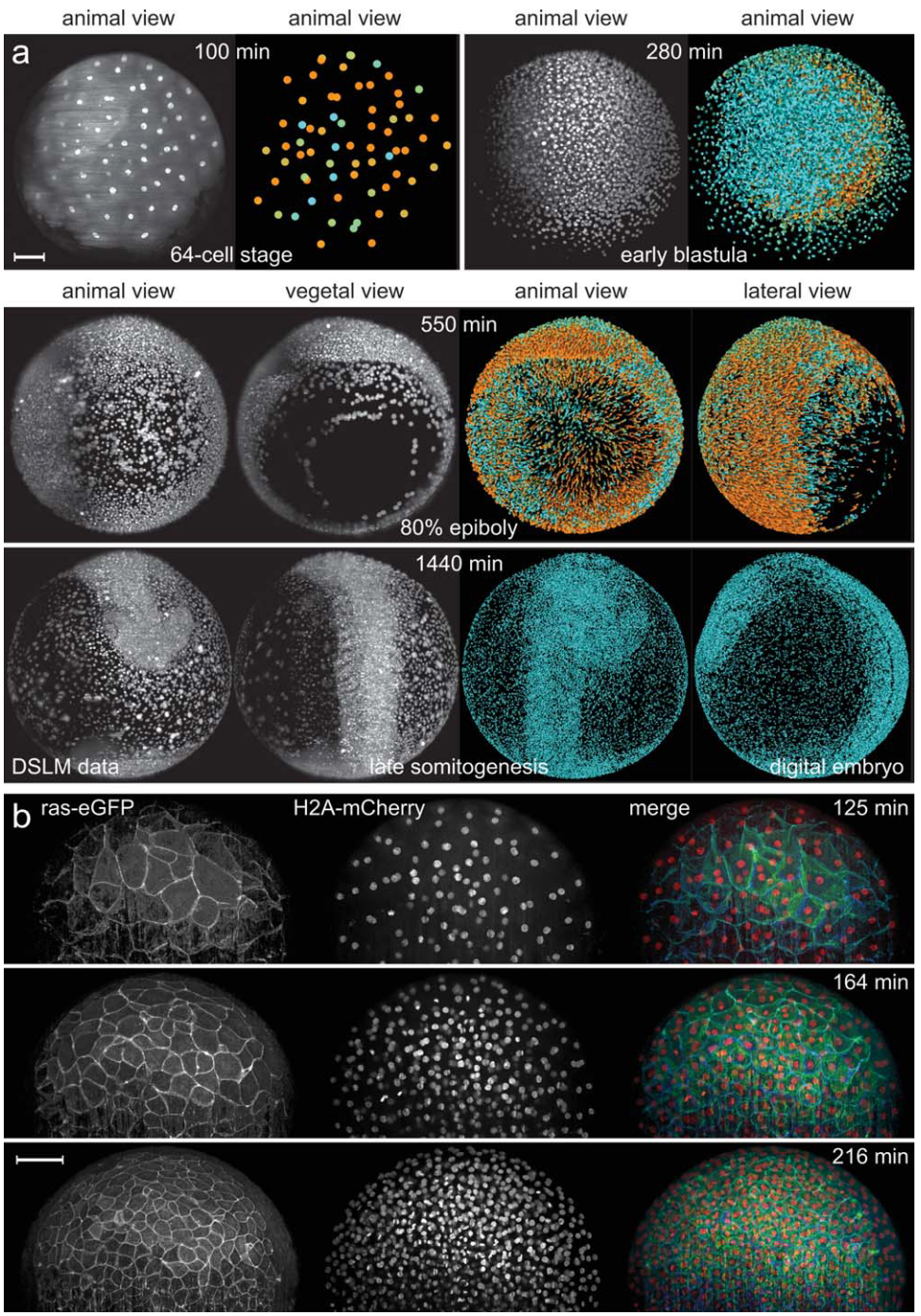

FIG. 4. Imaging zebrafish embryonic development with DSLM/DSLM-SI. (**a**) Maximum-intensity projections (left) and Digital Embryo reconstructions (right) of a nuclear-labeled wild-type zebrafish embryo at the indicated times and developmental stages. Color code: movement speeds (0 to 1.2 μm min^{-1}, cyan to orange). Images are deconvolved with Lucy-Richardson method (10 iterations). Scale bar, 100 μm. (**b**) Maximum-intensity projections of a DSLM time-lapse recording of a membrane- and nuclei-labeled zebrafish embryo injected with *ras-eGFP* mRNA and *H2A-mCherry* mRNA at the one-cell stage. Membranes were imaged using structured illumination (SI-25), and nuclei were imaged using standard light sheet illumination (LS). Images are deconvolved with Lucy-Richardson method (10 iterations). Scale bar, 100 μm. High-resolution movies are available at http://www.digital-embryo.org/. Credits: Panel (a) was reprinted from *Science*, vol. 322, Keller *et al*., "Reconstruction of Zebrafish Early Embryonic Development by Scanned Light Sheet Microscopy", 1065-1069, Copyright (2008), with permission from AAAS. Panel (b) was reprinted from *Nature Methods*, vol. 7 no. 8, Keller *et al*., "Fast, high-contrast imaging of animal development with scanned light sheet-based structured-illumination microscopy", 637-642, Copyright (2010), with permission from Macmillan Publishers Ltd.

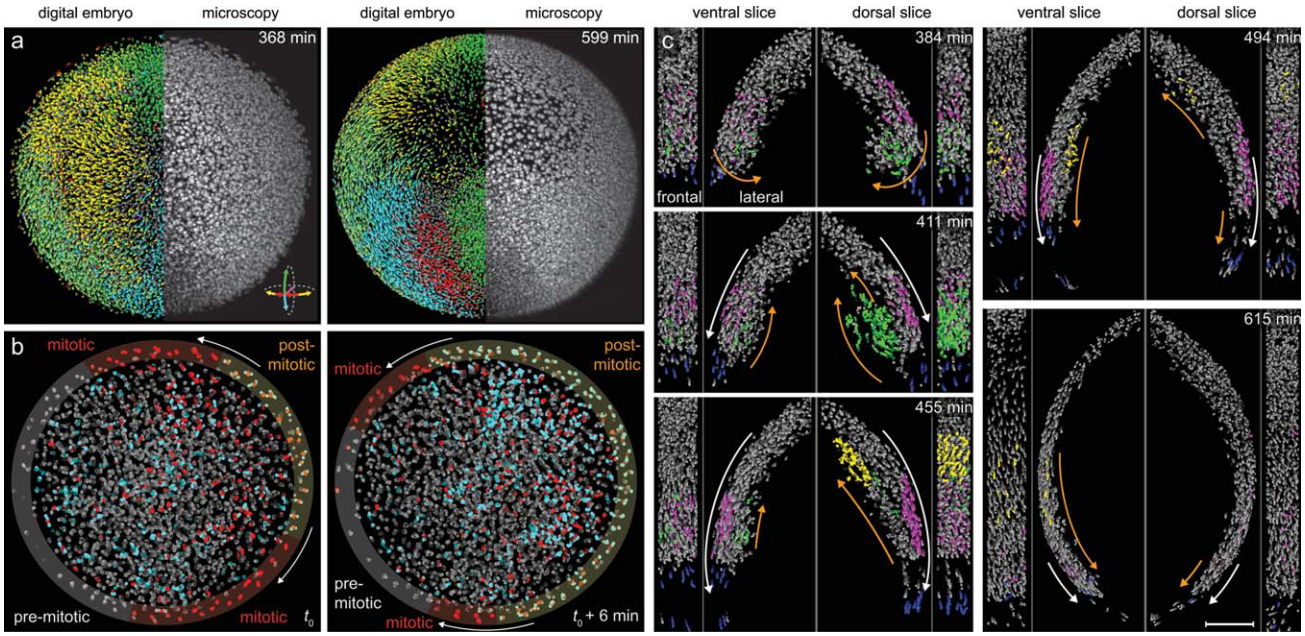

FIG. 5. Computational reconstruction of zebrafish embryonic development. (**a**) Detection of cell divisions in the Zebrafish Digital Embryo. Microscopy data (right half of embryo: animal view, maximum projection) and Digital Embryo (left half of embryo) with color-encoded migration directions. Color code: dorsal migration (cyan), ventral migration (green), toward or away from body axis (red or yellow), toward yolk (pink). (b) Cell tracking in the Zebrafish Digital Embryo. Dividing cells (red) and their daughter cells (blue). Yellow, red, and gray overlays indicate progression of the peripheral cell division waves during division cycle 12 (arrows show direction of peripheral waves; t_0 = 216 min post fertilization). (c) Mesendoderm internalization and migration in dorsal and ventral hemispheres. Frontal and lateral views of slices on dorsal (shield region, right) and ventral hemispheres (opposite of shield, left). Four cell populations were tracked: green or yellow nuclei in the early or late embolic wave, blue nuclei at the leading edge of epiboly, and noninternalizing pink nuclei. Orange and white arrows indicate hypoblast and epiblast cell movements. Scale bar, 100 μm. Databases and high-resolution movies of the Zebrafish Digital Embryo are available at http://www.digital-embryo.org/fish.html. Credits: Panels (a–c) were reprinted from *Science*, vol. 322, Keller *et al*., "Reconstruction of Zebrafish Early Embryonic Development by Scanned Light Sheet Microscopy", 1065-1069, Copyright (2008), with permission from AAAS.

image quality also in less transparent specimens, such as early *Drosophila* embryos, and allows optimizing image contrast in response to spatio-temporal changes of light scattering in the developing embryo (Keller *et al*., 2010). DSLM-SI was used to perform fast multiview imaging of *Drosophila* embryogenesis over 12 hours (Figure 6a), providing a data basis for the construction of a *Drosophila* Digital Embryo (Keller *et al*., 2010) (Fig. 6b, http://www.digital-embryo.org/fly.html).

Computational Techniques for the Study of Development

The fundamental goal of developmental biology is to understand how the fertilized ovum gives rise to the organism with all its complexity. The direct observation and quantification of this process by live microscopy is therefore an essential step. In contrast to "-omics" approaches, microscopy retains high spatial and temporal resolution (Megason and Fraser, 2007). However, the produced images are generally large and include many complex structures, which often make manual inspection and analysis impractical. Moreover, due to limitations inherent to the microscopy and labeling techniques, noise, low contrast and limited imaging depth complicate the analysis. What is required is a robust automated system that is able to analyze such data to provide comprehensive quantitative information about morphology and morphodynamics at cellular and subcellular levels. Such automation ensures efficiency, consistency, tractability, objectivity and completeness. The major process categories in this system are: (i) image restoration; to reconstruct the fluorescence signal and enhance contrast, e.g., deconvolution and multiview image registration and fusion, (ii) image analysis; to convert the voxel intensities into a more useful representation such as delineated objects, their tracks, higher order structures, or object annotations based on existing databases, (iii) modeling developmental processes; e.g., biophysical and mathematical modeling of developing tissue morphology and mechanics, which when combined with data analysis leads to image understanding (see Fig. 7). We will provide a quick survey on the above processes, highlighting noteworthy accomplishments and research directions relevant for advancing Quantitative Developmental Biology.

Image Restoration and Contrast Enhancement

The purpose of image post-acquisition processing is to increase contrast and/or to provide real-time feed-

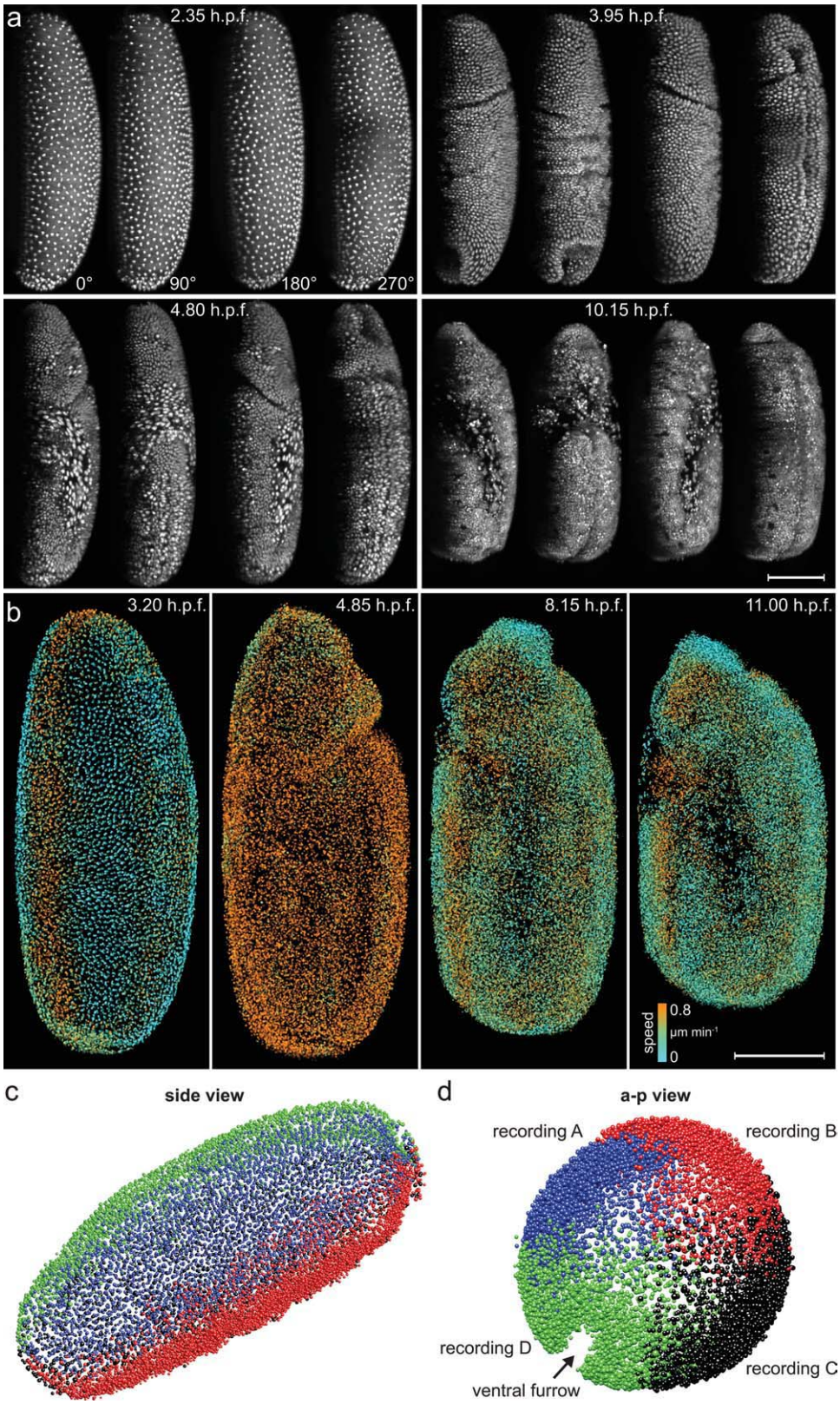

FIG. 6. Imaging and reconstructing *Drosophila* early embryogenesis with DSLM-SI. (**a**) Maximum-intensity projections of a DSLM-SI multiview time-lapse recording of a nuclei-labeled *Drosophila* embryo at the indicated times. Images are deconvolved with Lucy-Richardson method (five iterations). (**b**) Lateral snapshots of the *Drosophila* Digital Embryo. Colored spheres represent the nuclei that were automatically detected in the DSLM-SI microscopy recordings of the developing *Drosophila* embryo. Colors indicate directed regional nuclei movement speeds over 10-min periods. Scale bars, 100 μm. (**c/d**) Multiview fusion of the *Drosophila* Digital Embryo. Alignment of the four point clouds representing the nuclei detected in the four views of the developing *Drosophila* embryo. Nuclei shown in different colors originate from different microscopic views. Side view (**c**) and view along the anterior-posterior axis of the embryo (**d**). Databases and high-resolution movies of the *Drosophila* Digital Embryo are available at http://www.digital-embryo.org/fly.html. Credits: Panels (a-d) were reprinted from *Nature Methods*, vol. 7 no. 8, Keller *et al*., "Fast, high-contrast imaging of animal development with scanned light sheet-based structured-illumination microscopy", 637-642, Copyright (2010), with permission from Macmillan Publishers Ltd.

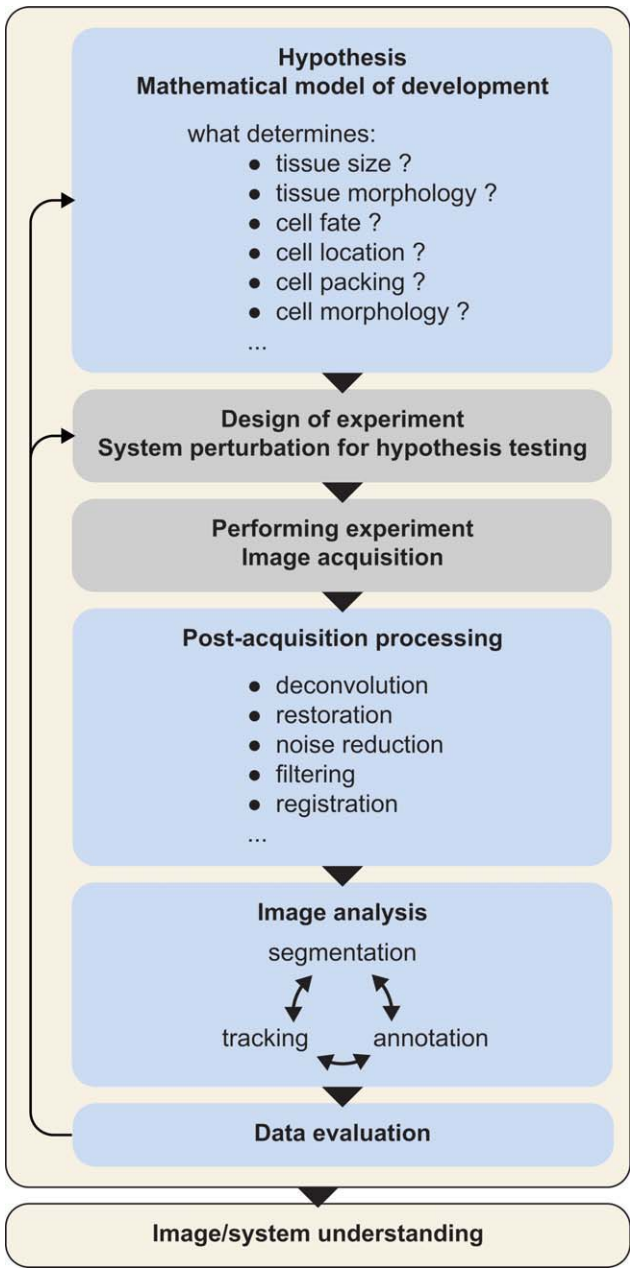

FIG. 7. A general scheme for system understanding based on microscopy data analysis is composed of iterations of hypothesis testing. After image acquisition, image post-acquisition processing (image restoration) is performed; this typically includes image deconvolution, noise filtering, edge enhancement, image registration and fusion. This is followed by the core image analysis tasks. Common tasks are parsing images (image segmentation) for labeled objects such as cells and nuclei, generation of tracks over time, as well as higher level analysis to identify e.g., lineages and cell types. The output of the image analysis is typically compatible with the mathematical model and is used as a test for its predictive power. The last step is refining the model based on the output from the image analysis. Models are then iteratively tested and refined by perturbing the experimental system and designing new experiments.

back to the microscope system. Image deconvolution, registration, and fusion are all tasks that lead to this goal. The importance and details of post-acquisition processing depend on its degree of integration with the microscopy as well as the required subsequent data analysis. So for example, widefield microscopy provides high image acquisition speeds. However, to achieve optical sectioning, the computational task of deconvolution is necessary. Traditionally, deconvolution estimates the original unobserved object using the blurred observed image and the microscope's point spread function (or an estimate of it) (Lucy, 1974; Markham and Conchello, 1999). It is still a slow iterative process that requires large amounts of computer power, despite ongoing improvements (Hom *et al.*, 2007; Lam and Goodman, 2000). Therefore, the common strategy is to couple high-speed widefield acquisition with offline deconvolution (Racine *et al.*, 2007). Several deconvolution software packages exist and are commonly applied, including commercial (Autoquant by Media Cybernetics and Huygens by Scientific Volume Imaging) and noncommercial (Aida (Hom *et al.*, 2007) and BiaQIm (http://www.bialith.com/)) solutions.

Since most image analysis tasks provide more accurate results when spurious structures are suppressed and edges are enhanced, image enhancing and noise reducing filters should be applied when appropriate. Common examples are anisotropic diffusion (Perona and Malik, 1990), median filtering and Gaussian blurring. For a recent survey and comparison of methods in the context of zebrafish imaging see Kriva *et al.* (2010). A word of warning: care must be taken, since these filters will change pixel and voxel intensity values. Tasks, for which the original intensity values (or relative intensity values) are important, such as correlation, should be performed without application of such filters.

Image Registration

Image registration transforms an image (called the source) into the coordinate system of a reference image according to some overlap metric. This computationally demanding process is required when comparing images across different view angles, specimens, or time points. It is often a prerequisite for further analysis steps such as image fusion, tracking and cell annotation. Generally, an image registration system is composed of three components: (1) a similarity metric that measures the extent of overlap of the source image with a reference image, (2) a transformation model, i.e. a mechanism for performing rigid, affine or freeform transformations, and (3) an optimization engine that maximizes the overlap of source and reference by fitting transformation parameters. Image registration is commonly applied in a multiresolution strategy to reduce computational load. The

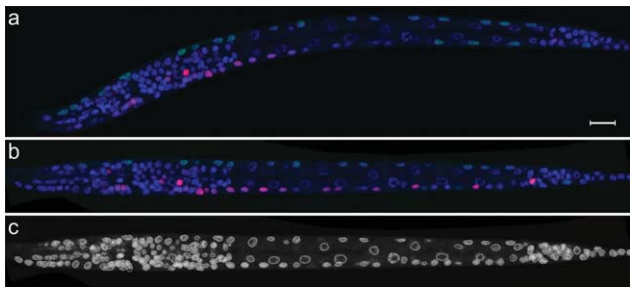

FIG. 8. Automated image processing of fluorescence images of *C. elegans* larvae. (**a**) A two-dimensional slice of the three-dimensional image stack. Blue, DAPI; green, nuclear localization signal (NLS)-GFP expressed from the *myo*-3 promoter; red, mCherry regulated by a promoter of interest (in this example, expression is in some ventral motor neurons and neurons in the nerve ring). Scale bar, 10 μm. (**b**) The same two-dimensional slice after worm body straightening. (**c**) The segmentation result of the DAPI channel of same three-dimensional image, with the same two-dimensional slice as in (a). Credits: Panels (a–c) were reprinted from *Nature Methods*, vol. 6 no. 9, Long *et al*., "A 3D digital atlas of *C. elegans* and its application to single-cell analyses", 667-672, Copyright (2010), with permission from Macmillan Publishers Ltd.

main idea is to perform rough registration on downsampled images and to refine the registration stepwise as the resolution is digitally increased up to that of the original data. In addition, image registration may be intensity-based, i.e., at the voxel level, using image correlation metrics (Liu *et al*., 2009b; Long *et al*., 2009; Peng *et al*., 2008; Swoger *et al*., 2007; Tomer *et al*., 2010) or feature based (Al-Kofahi *et al*., 2002; Fowlkes *et al*., 2008; Keller *et al*., 2010; Mace *et al*., 2006; Peng *et al*., 2008; Preibisch *et al*., 2010; Sun, 1989), in which case the registration is reduced to point or feature matching. There is an extensive literature on image registration (see Brown (1992) and Zitova (2003) for comprehensive reviews). Especially in the medical imaging field, accurate efficient registration is critical for computer-aided diagnostics, and in this context most of the early image registration methods have been developed.

Biological image registration is also being increasingly applied in the context of tissue morphogenesis. Tomer *et al*. (2010) used a sophisticated and powerful combination of intensity-based registration methodologies to establish homology between development of the vertebrate pallium and the sensory-associative brain centers in an annelid. They used a combination of rigid, affine, and nonrigid transformation models in a multiresolution analysis. Peng *et al*. (2008) developed a novel nonrigid feature-based technique to straighten *C. elegans* worms (the worm straightening algorithm—WSA, Fig. 8). Their strategy was to reduce the worm representation to a one-dimensional manifold by determining the anterior-posterior axis. They constructed the straightened image as a series of one-pixel separated planes perpendicular to the one-dimensional line by image rotation. This approach lies in sharp contrast to landmark-based three-dimensional nonrigid registration methods, in which a deformation field is calculated. WSA has found application in the automated determination of *C. elegans* cell fates by gene expression profiling (Liu *et al*., 2009b). Fowlkes *et al*. (2008) built a quantitative spatio-temporal atlas for gene expression in the *Drosophila* blastoderm (the model VirtualEmbryo—Fig. 2) using point cloud registration as their primary tool.

For the registration of multiview light sheet microscopic images a Fourier-domain technique has been implemented (Swoger *et al*., 2007), as well as a point-cloud method that relies on segmenting beads acting as fiducials (Preibisch *et al*., 2010).

Another type of application that can benefit from image registration is time-lapse imaging. Large tissues or groups of cells may move out of the field-of-view during the acquisition. To maintain detailed observation, automatic registration from one frame to the next is used to calculate a transformation that guides the microscope stage to keep the desired part of the sample in the field of view in an adaptive manner (Rabut and Ellenberg, 2004).

Image Analysis

Image analysis converts voxel intensities into usable information such as cell boundaries, geometries, spatial organization, and trajectories. Automation of image analysis is essential to avoid subjective results and to handle large datasets. Current efforts increasingly focus on developing robust high-throughput image analysis systems. See for example recent studies on the development of zebrafish (Brown *et al*., 2010; Campana *et al*., 2010; Campana and Sarti, 2010; Keller *et al*., 2008b; Liu *et al*., 2008; Melani *et al*., 2007; Rizzi *et al*., 2007; Rizzi and Sarti, 2009; Zanella *et al*., 2010; Zanella *et al*., 2007), *Drosophila* (Frise *et al*., 2010; Keller *et al*., 2010; Keranen *et al*., 2006; McMahon *et al*., 2008; Peng *et al*., 2007; Supatto *et al*., 2009; Weber *et al*., 2009; Zhou and Peng, 2007) and *Arabidopsis* (Fernandez *et al*., 2010) (see Fig. 9). By far the most prominent image analysis task is image segmentation, which we present in some detail (see Table 1 for an overview of some recent studies). It converts data from a pixel-based representation to an object-based one. Image segmentation is a prerequisite for further analyses, as can be seen in recent studies focusing on cell tracking (Brown *et al*., 2010; Jaqaman *et al*., 2008; Keller *et al*., 2008b; Supatto *et al*., 2009), tissue tracking (Zamir *et al*., 2005), lineaging (Bao *et al*., 2006; Fernandez *et al*., 2010; Hirose *et al*., 2004; Murray *et al*., 2006; Olivier *et al*., 2010) and annotation of cell type or cell cycle state (Held *et al*., 2010; Long *et al*., 2009).

Image Segmentation

Image segmentation (or just segmentation) is the process of delineating cellular and other labeled boundaries, yielding their numbers, position and geometries. It

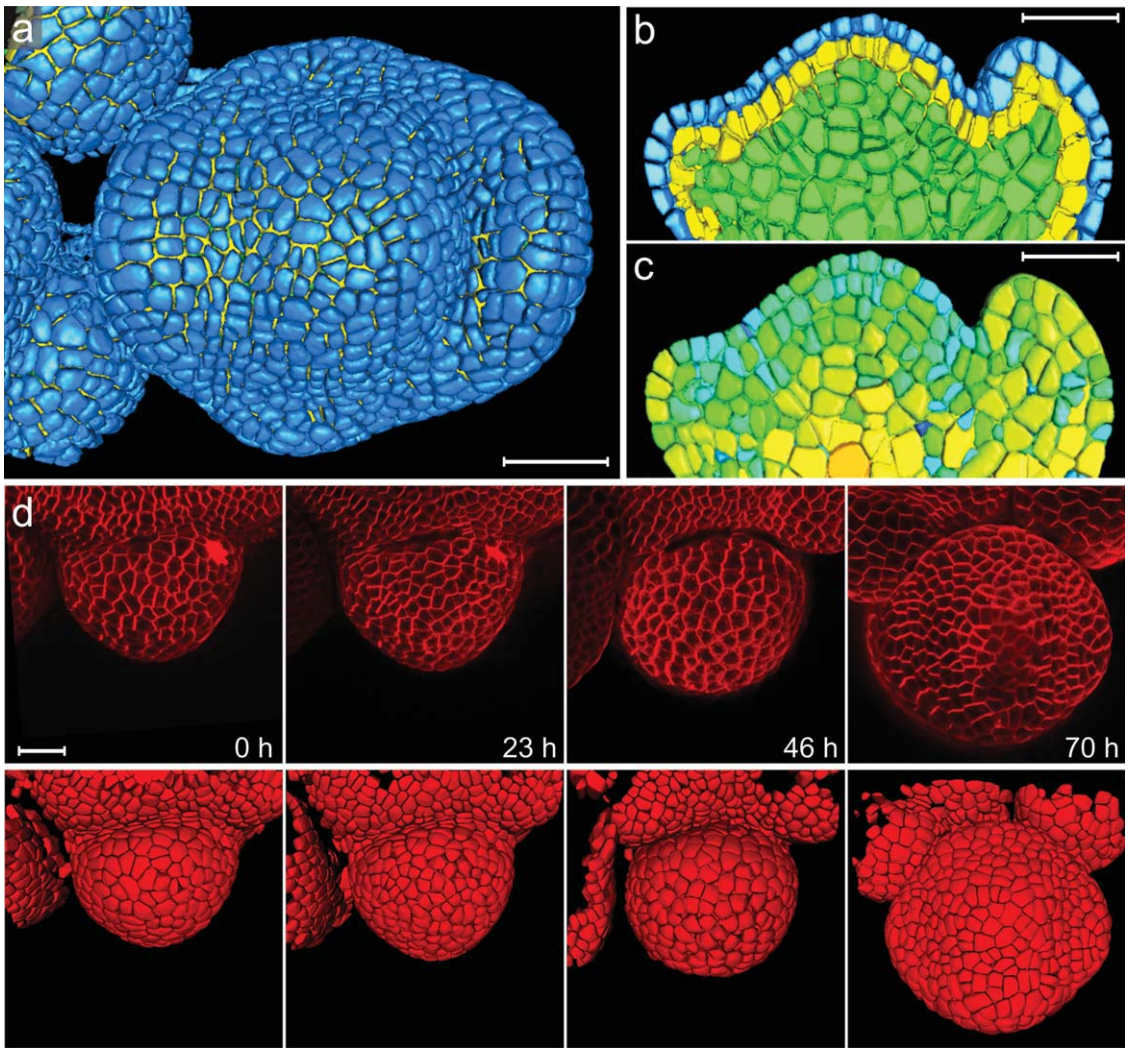

FIG. 9. Reconstructing plant development. (a) Multiangle image acquisition, three-dimensional reconstruction and cell segmentation (MARS) of *Arabidopsis thaliana*. After automatic segmentation, the tissue was visualized with a full organ reconstruction. Scale bar, 50 μm. (**b/c**) Virtual tissue sections using color codes for cell layer (b) or cell volume (c). Scale bar, 25 μm. (**d**) Upper row: Confocal image surface projections of the top view of a wild-type flower collected at the indicated times. Lower row: Segmented three-dimensional reconstructions of each time point (corresponding to images in the upper row). Credits: Panels (a–d) were reprinted from *Nature Methods*, vol. 7 no. 7, Fernandez *et al*., "Imaging plant growth in 4D: robust tissue reconstruction and lineaging at cell resolution", 547-553, Copyright (2010), with permission from Macmillan Publishers Ltd.

is an essential task preceding many other image analysis steps and represents one of the grand challenges of computer vision (Szekely and Gerig, 2000). In particular developmental biology can benefit from advances in this field, since imaging live developing organisms leads to data that is difficult to analyze manually. Variations in fluorescence marker expressions, morphological complexity, tight packing of cells as well as light scattering and shadowing effects complicate image segmentation and can considerably decrease the accuracy of traditional techniques.

We will quickly touch upon the main classes of computational image segmentation algorithms, and will then highlight how, and in which context, some of these approaches have been successful in the study of morphogenesis. There are several ways in which segmentation algorithms can be classified, for example, supervised vs. unsupervised, intensity-based vs. gradient-based, model-based vs. low-level. Also some algorithms are more suitable for "blob-object" segmentation (such as cell and nuclear lumen-labels), while others are tailored for detecting the cell boundary (for example membrane labels). We present a classification according to the general computational complexity of the algorithm and provide comments on other aspects as well.

Table 1
Overview of Some Recent Approaches to Image Segmentation in Developmental Biology

Reference(s)	Model	Application	Microscopy	Segmentation method
Al-Kofahi *et al*. 2006	Mouse (*in vitro*)	Segmentation of neural cell outlines	Phase contrast	Adaptive thresholding, followed by watershed
Bao *et al*. 2006	Nematode	Segmentation of nuclei throughout embryogenesis	Confocal fluorescence	Shape prior, assuming spherical nuclei
Fernandez *et al*. 2010	Thale cress Rice roots	Segmentation of cell membranes in flowers and roots	Confocal fluorescence	Watershed
Keller *et al*. 2008b	Zebrafish	Segmentation of nuclei during early embryogenesis (1–24 hpf)[a]	DSLM	Iterative adaptive thresholding
Keller *et al*. 2010	Fruit fly	Segmentation of nuclei during early embryogenesis (1–12 hpf)[a]	DSLM-SI	Laplacian-of-Gaussian blob detection, followed by machine learning-based clustering of detected centers
Li *et al*. 2007a Li *et al*. 2008a	Zebrafish	Segmentation of nuclei in different stages and tissues	Confocal fluorescence	Diffusion gradient vector field, followed by gradient vector flow tracking
Long *et al*. 2009 Liu *et al*. 2009b	Nematode	Segmentation of nuclei in L1 larvae	Confocal fluorescence	Adaptive thresholding, morphological operators, 3D watersheds and support vector machine classifier
Luengo *et al*. 2006 Fowlkes *et al*. 2008	Fruit fly	Segmentation of nuclei in early embryos	Multiphoton fluorescence	Watershed-based with shape priors
McMahon *et al*. 2008 Supatto *et al*. 2009	Fruit fly	Segmentation of nuclei during gastrulation	Multiphoton fluorescence	Imaris spot segmentation
Olivier *et al*. 2010	Zebrafish	Segmentation of cell membranes in early embryos (1–3 hpf)[a]	Second-/Third-harmonic generation	Watershed-based
Yu *et al*. 2009a Yu *et al*. 2010	Mouse (*in vitro*)	Segmentation of cell membranes and nuclei in neurospheres	Widefield fluorescence	Level-set, combined with topological priors
Zanella *et al*. 2010	Zebrafish	Segmentation of cell membranes and nuclei in early embryos	Confocal and multiphoton fluorescence	Subjective surfaces

[a]hpf, hours post fertilization.

Thresholding

Threshold-based algorithms find an intensity value above which all voxels belong to the foreground (object) and the rest is background. They are the computationally most efficient strategies. The main assumption is that all desired features can be discerned based on intensity, and, for automatic algorithms, that all information necessary for finding the appropriate threshold is contained in the image itself.

Global thresholding is the simplest strategy. The user or algorithm selects an intensity value $\min(f(x)) < t < \max(f(x))$, with f(x) representing the intensity information constituting the image. The binary segmented image voxels are set to one for all $f(x) > t$, and zero otherwise. t can be chosen manually, or based on priors such as the expected volume of the segmented object(s). A widely used automatic method for choosing t is Otsu's method (Otsu, 1979), which calculates the optimum threshold separating fore- and background voxel classes such that their combined intraclass variance is minimal. More recent methods include the stable count threshold (Russel *et al*., 2009) and fuzzy sets (Tobias and Seara, 2002).

Thresholding is computationally very efficient, but only yields good results when structures are well separated and contrast is uniform and high (MacAulay and Palcic, 1988). It is often used to provide a starting guess for more sophisticated approaches.

Edge Detection

Closely related to thresholding, edge detection methods operate on the derivative of the image instead of its intensity. The assumption is that object boundaries are located in regions where intensity changes are abrupt. Well known edge detector algorithms include Laplacian-of-Gaussian (Marr and Hildreth, 1980), Sobel (Sonka *et al*., 1998), and Canny (Canny, 1986). These algorithms try to find edge pixels while eliminating the effect of noise. Although edge detection algorithms are fast, structures are output as discrete edge voxels, and may be incomplete or discontinuous. Post-processing is generally necessary to obtain closed contours. Also, despite much ongoing research, edge detection algorithms are highly sensitive to noise.

Region Growing

The main idea of region growing algorithms is that all voxels belonging to the same object are (a) connected (according to some neighborhood criteria), and (b) fulfill some binary quality function Q. A general region growing algorithm will usually start at some seed point(s) (found for example by thresholding) and check immediate neighbors for fulfilling Q. Voxels for which Q is equal to one will be added to the region, and the next iteration is initiated. Iterations commence until no neighbors are added. Region growing algorithms differ mainly in their implementation of Q. The simplest strategy is growing according to voxel intensity value. The object's gray values are assumed to be within some range around a mean value. So neighbor voxels are added, if their intensity value lies within some range around the region's mean. Variants on region growing algorithms include adaptive region growing (Modayur *et al*., 1997), in which the decision to add a new neighbor is weighted by how close the region has reached an expected size (note the inclusion of prior knowledge), competitive region growing (Adams and Bischof, 1994), nonconnected region growing (Revol and Jourlin, 1997) and region growing strategies that do not require initial seed points (Revol-Muller *et al*., 2002).

Region growing algorithms are computationally intensive, noise leads to over-segmentation and hole-formation, and they only separate the regions that share the property defined in Q. Nevertheless, they are flexible in the choice of (multiple) criteria, are based on a simple concept and are easy to program on a computer.

Pattern Recognition

Volumetric images can be regarded as patterns subject to pattern classification algorithms, which can generally be classified into supervised and unsupervised ones. Supervised methods include supervised artificial neural networks (Alirezaie *et al*., 1997), support vector machines (Wang *et al*., 2001) and active shape models (Cootes *et al*., 1995). A training set is needed for all of these methods. The first two are nonlinear statistical data modeling tools. They can model complex relationships between inputs and outputs. Active shape models encode the variability of shapes from an appropriate training set using selected shape parameters. The method depends on a good parametric model that encodes the most important morphological features. Segmentation proceeds by finding the best position of the shape points according to the appearance information. Active shape models are closely connected to deformable models (described below) due to the necessity of an economic shape description.

Another popular technique is k-nearest neighbors classification (Duda and Hart, 1973). It can be used to estimate a tessellation of the feature space leading to classification of the entire image. The disadvantage is that it handles voxels in the image independently, and additional machinery, for example Markov random fields (Li, 1995) or mathematical morphology (Serra, 1982), needs to be implemented to define the spatial correlation between single voxels.

In the unsupervised pattern recognition procedures (also called clustering algorithms) no training set is needed. Those are variants of the k-means algorithm. For example the fuzzy c-means algorithm (Mohamed *et al*., 1999) iteratively minimizes the intracluster variation. Vox-

els are classified according to a weighted distance function to the nearest cluster centroid. The cluster centroid is updated and the voxels reassigned. The algorithm terminates when all voxels have been classified.

Pattern recognition techniques can greatly enhance image segmentation accuracy. Their application has been mainly limited to the medical imaging field. However, the supervised algorithms are expected to become more important for the life sciences as more representative morphological data is produced and large accurate training sets can be constructed.

Watershed Transform

The watershed transform (Vincent and Soille, 1991) considers the image as a system of catchment basins. A catchment basin is the set of all voxels from which the path of steepest descent ends in the same voxel. These basins are "flooded" at the local intensity minima, thus subdividing the image into regions and delimiting contours. During the course of associating voxels with basins, contiguous neighborhoods are given identical labels. At the regions where voxels would be associated with multiple basins, watersheds exist, and a "dam" should be built.

Watersheds always produce closed contours, however they generally yield over-segmentations, and variants of the algorithm include strategies to overcome this limitation (Bleau and Leon, 2000). For a critical survey and review see Roerdink and Meijster (2001).

Deformable Models and Level Sets

Low-level techniques (e.g., thresholding, edge detection, region growing, and *k*-means clustering) generally assume that the segmentation can be carried out based on information inherent to the image. This assumption is fundamentally wrong (Szekely and Gerig, 2000). Especially for the rich image data produced with modern microscopes, low-level techniques—though CPU efficient—will not be able to generally produce satisfactory segmentations. Incorporation of even rudimentary prior knowledge is enough to increase the accuracy of the segmentation. An important example of such a prior is the assumption that imaged structures such as organelles, cells or tissues are smooth, or bounded by a biological membrane, and thus subject to physical constraints of bending and tension energies. We can therefore describe the structures computationally using direct surface representation methods. Segmentation proceeds in the image domain by the evolution of these contours formulated in terms of the minimization of an energy functional. This is the technique of deformable models (Moore and Molloy, 2007; Terzopoulos and McInerney, 1997). It has received much attention recently in the context of segmenting medical and biological images (Chang *et al*., 2007; Debeir *et al*., 2004; Degerman *et al*., 2009; Dormann *et al*., 2002; Dufour *et al*., 2005; Khairy *et al*., 2008a; Khairy and Howard, 2008; Khairy *et al*., 2008b; Li *et al*., 2008b; McInerney and Terzopoulos, 1996; Mukherjee *et al*., 2004; Padfield *et al*., 2009a; Padfield *et al*., 2009b; Pecreaux *et al*., 2006; Ray *et al*., 2002; Shen *et al*., 2006; Zimmer *et al*., 2002). Deformable models can be classified into parametric and geometric models (Sonka *et al*., 1998).

Parametric models are usually associated with the snake method (Kass *et al*., 1988). The surface is represented explicitly, for example as a set of connected surface points (triangular mesh) or compactly in the form of coefficients of a series expansion (Brechbühler *et al*., 1995; Khairy and Howard, 2008; Khairy *et al*., 2008b; Styner *et al*., 2005) (for a survey of shape representation methods for deformable models see (McInerney and Terzopoulos, 1996)). Associated with the surface is an energy functional composed of internal (image independent) and external (image dependent) energies. The internal energy includes shape priors. It keeps the contour smooth, and is defined through geometric properties of the contour such as surface area and curvature. This energy can be directly related to known biophysical measurements such as the rigidity of the biological membrane and its surface tension (Pecreaux *et al*., 2006). The external energy is a measure of how accurately the contour overlaps with features in the smoothed image (or its derivative). The main idea is to construct an Euler-Lagrange equation, with a time variable, based on the energy functional. The contour is evolved in time until equilibrium is reached. According to the definition of the Euler-Lagrange equation, equilibrium is the balance between internal and external energies, and would result in a contour that is generally smooth (conforms to priors) and simultaneously represents the structure in the image (conforms to the data). The first implementation of this idea—the snake method—was sensitive to the starting position of the contour because it depended on image gradient. This means that parts of the contour had to "feel" the pull of the gradient to converge. Later improvements of the algorithm successfully decreased the dependence on starting configurations and noise (Cohen, 1991; McInerney and Terzopoulos, 1995; Xu and Prince, 1998). An important example of these methods is the highly successful diffusion gradient vector field approach (Xu and Prince, 1998). This method was adapted to a contour-free version (Li *et al*., 2008a; Li *et al*., 2007b) that has found recent application in zebrafish nuclei segmentation (Li *et al*., 2007a). Other variants of deformable model methods do not use curve evolution, but perform a direct numerical minimization of the curve-associated energy (Khairy and Howard, 2008) or alternatively Markov Chain Monte Carlo optimization within a statistical Bayesian inference framework (Khairy *et al*., 2008b). Importantly, paramet-

ric deformable models provide a way to incorporate prior information in a flexible manner, and with only moderate loss of computational efficiency.

A limitation of parametric deformable models is that they cannot handle topological changes without extra computational machinery. This is naturally solved by geometric deformable models, which are based on the level set method (Osher and Sethian, 1988). The main idea is to implicitly embed the evolving contour into a higher dimensional function and view the contour as its zero level. The advantage is that normals and curvatures of the contour can be efficiently calculated just as in the parametric models, but with the added advantage of the natural handling of topological changes. Therefore the computational complexity is decreased when segmenting many independent objects simultaneously. In particular the geodesic active contour (Caselles *et al*., 1997) and Chan and Vese (2001) models are widely used. The former is recommended when objects have clear boundaries and the latter when it is difficult to discern the transition from object to background. We should state here that the free change in topology is not always desired, and one must carefully choose the algorithm based on the particular dataset at hand.

In contrast to the popular watershed transform (see above) deformable model algorithms tend to undersegment the image by merging objects that are closely situated in the image. This requires some post-processing to refine the results. Nevertheless, the high flexibility of the method and the close connection to biophysics make deformable models an excellent candidate as a quantitative image analysis technique in developmental biology.

Practical Image Segmentation in Developmental Biology

The above techniques represent the main classes of algorithms for image segmentation. Recently, some variants of them have been successfully applied to the problem of segmenting fluorescence images in developmental biology studies (Table 1). The endeavors can generally be classified into nuclei and cell membrane segmentation. Segmentation of cell nuclei, i.e., in the presence of a nuclear label, is easier since nuclei typically exhibit more uniform shapes and fluorescence intensity levels. They are also better separated. To mention a few recent studies; Al-Kofahi *et al*. (Al-Kofahi *et al*., 2006) used adaptive thresholding followed by watershed transform for segmentation of mouse neural progenitor cells growing in culture. They used their results as input for automated lineage construction. Bao *et al*. (Bao *et al*., 2006) reconstructed *C. elegans* cell lineages from fluorescence recordings of specimens with GFP-labeled histones. For the initial segmentation of nuclei, they used low-pass filtering and histogram-based thresholding. This was followed by determination of local intensity maxima identification to determine positions of nuclei. They incorporate priors about the approximate size and spacing between nuclei to determine approximate nuclear geometries. Keller *et al*. (2008b) developed an adaptive iterative thresholding method, which was used to construct the Zebrafish Digital Embryo (Figs. 4 and 5). McMahon *et al*. (McMahon *et al*., 2008; Supatto *et al*., 2009) used the spot segmentation method of the commercial software Imaris to investigate collective cell migration in *Drosophila* (see Fig. 1). Keller *et al*. (2010) applied a Laplacian-of-Gaussian blob detection-based method for determining nuclear centers from DSLM-SI data of developing *Drosophila* embryos. This was followed by estimation of nuclear diameters from the local intensity distributions, and led to the generation of the *Drosophila* Digital Embryo (Fig. 6).

Image segmentation algorithms that find cell boundaries, even when cells are touching, are critical for developmental biology. Although there are many specific fluorescent membrane labels, the recorded boundaries are often incomplete and their quality depends on the specific dye used, expression levels and depth of observation. The subjective surfaces method (Sarti *et al*., 2000) reconstructs incomplete boundaries, and—in combination with post-acquisition filters—has been implemented for zebrafish cell boundary segmentation (Zanella *et al*., 2010). Another technique for cell boundary detection has been developed based on finding the gray-weighted distance transform (Baggett *et al*., 2005). The approach is promising, as its extension to three dimensions is straightforward. The recently developed Evolving Generalized Voronoi Diagrams (EGVD) method (Yu *et al*., 2010) utilizes intensity, geometric information and topological constraints to segment touching cells within a one-function level-set approach. Its generalization to three dimensions is also straightforward (Yu *et al*., 2009b), and has been used in the study of mouse neuroblastoma neurite outgrowth (Yu *et al*., 2009a).

In general, cell boundary segmentation from images of fluorescently labeled membranes is challenging and computationally demanding, and is still the focus of a number of current efforts.

Summary of Image Segmentation

A universal solution for the problem of image segmentation is not feasible, and progress in this field has been rather slow (Pavlidis, 1992; Zamperoni, 1996). Effectively, there are as many segmentation strategies as there are segmentation problems (see Table 1 for an overview of some recent approaches in the context of developmental biology). The human visual system is able to perform segmentation easily and quickly, while for computers segmentation is a difficult problem as it

is ill-posed. Well-posed problems have solutions that (1) exist, (2) are unique, and (3) change smoothly with small changes in the data. In the case of image segmentation, we assume that the first criterion is satisfied. However, to satisfy points (2) and (3), we need to introduce prior knowledge, whose details will strongly influence the result of the segmentation. In general, low-level algorithms make no assumptions about the objects and yield inferior segmentations. At the other extreme are correlation and covariance methods (template matching), in which the object sought is of precisely known shape or exhibits precisely known properties and the computer searches for these in the data. In between are algorithms that take advantage of prior knowledge to different degrees; in increasing order: region growing, deformable models and Hough transform (and its variants). The most flexible framework to express prior knowledge for image segmentation is Bayesian inference. Many segmentation algorithms can be formulated in Bayesian terms, e.g., thresholding, deformable models, and Markov random fields.

Cell Tracking and Lineaging

Once the cells or nuclei have been segmented over time, we can follow collective cell migration and perform lineaging and cell annotation. To reach that goal, cell tracks must first be generated by associating each segmented cell (or nucleus) with a track.

The simplest strategy is to associate each cell centroid in a frame to the spatially closest one in the next frame. This is accurate when cell movements are slow in relation to imaging speed. When this is not the case, accuracy of tracks can be increased by generalizing the concept of "distance" between cells to that of a feature vector, which includes details of the morphology (e.g., in the form of Fourier shape coefficients), fluorescence intensity, volume, surface area, or total curvature (bending energy).

Also, segmentation methods can be extended to cell tracking; examples are template matching between one frame and the next, or deformable models segmentation, in which the contour extracted from one frame serves as the starting guess for segmentation in the next one. Correlation analysis can provide accurate identities for tracking when contrast and temporal resolution are high (Brown *et al*., 2010; Keller *et al*., 2008b) (Figs. 4 and 5). More sophisticated methods include gradient vector flow (Ray *et al*., 2002; Zimmer *et al*., 2002) and estimated cell dynamics (Debeir *et al*., 2004; Shen *et al*., 2006). Liu *et al*. (2009a) use a graph matching method (Gold and Rangarajan, 1996) for tracking plant cells in noisy images. They exploit the local tissue structure, incorporating relative position information of cells with respect to their neighbors. Some probabilistic approaches are also promising (Cui *et al*., 2006; Kachouie *et al*., 2006; Li *et al*., 2008b; Shen *et al*., 2006). In the context of developmental biology, Al-Kofahi *et al*. (2006) developed an effective prior knowledge tracking strategy based on evaluating probabilities of whether cells move, divide or die between consecutive image frames. They separate the task of cell segmentation from the matching algorithm. Matching decisions are based on the solution of a numerical integer programming problem. Their method is able to recognize and isolate errors in the initial segmentation during the track assignment stage; however a training set is needed for setting method-specific parameters. Also noteworthy is the fuzzy soft-assign algorithm (Chui and Rangarajan, 2003) developed for point-set matching and based on deterministic annealing (Rose, 1998). It was modified for cell tracking (Gor *et al*., 2005) by extension to problems with one-to-many correspondences. Other recent examples for tracking and lineaging are shown in England *et al*. (2006), McMahon *et al*. (2008) (see Fig. 1), Fernandez *et al*. (2010) (see Fig. 9) and Olivier *et al*. 2010).

Lineaging Software

The most commonly used program for generating lineages is SIMI BIOCELL (Schnabel *et al*., 1997), which, however, involves a significant amount of manual intervention. Specific for lineaging of *C. elegans* is Angler (Martinelli *et al*., 1997), which browses images of the worm embryo during early development and relates these images to overlaid cell lineage data and three-dimensional schematic views of cell positions. A general lineage determination algorithm is StarryNite (Bao *et al*., 2006; Murray *et al*., 2006), which segments nuclei in a semisupervised fashion, traces them in time and assigns daughters to mothers. The developers of StarryNite also developed the program AceTree, which serves as a lineage editor to correct errors, and to visualize and compare lineages.

Visualization and Annotation in Developmental Biology

The need for integrated computer programs that a biologist can run on a personal computer to study development, has led to the generation of software systems that streamline cell annotation and data visualization. Heid *et al*. have developed the 3D-DIASemb program (Heid *et al*., 2002) integrating tracking, visualization of whole embryos and analysis of cytoplasmic flow. Their software requires the segmentation to be performed in a semiautomatic way (whole embryos are found automatically, and segmentation of cells and nuclei is done manually). Tassy *et al*. developed the 3D virtual embryo software (Tassy *et al*., 2006) for cell annotation, which was demonstrated on a fixed sample. The input to their system is a segmentation performed

separately, and for which they used commercial software. Fowlkes *et al*. (2008) developed the program PointCloudXplore which allows visualization of quantitative three-dimensional expression data (Fig. 2b). The user can interactively explore average regulatory relationships between multiple genes (http://bdtnp.lbl.gov/Fly-Net/bioimaging.jsp). Peng *et al*. (2009) developed the software VANO for volume-object image annotation. The user can visualize and annotate 3D volumes starting with either raw image data or a presegmentation. Objects can be labeled, categorized, deleted, added, split, merged and redefined. VANO was applied to build and annotate high-resolution digital atlases of the cells in *C. elegans* larvae and neuronal patterns in the adult *Drosophila* brain.

More recently the problem of visualization in 4D datasets (space plus time) has been addressed. The main challenge here is the large size of the datasets and the need for interactivity. Campana and Sarti (2010) developed a distance-map driven real-time volume rendering system that takes advantage of modern GPU architecture. They demonstrate their approach on time-lapse recordings of zebrafish development. Also, a powerful cross platform program for real-time visualization of large image datasets is the V3D software of Peng *et al*. (2010). Their system can be customized with plug-ins to address specific biological questions, and has been used to build a three-dimensional atlas of neurite tracts in the *Drosophila* brain (http://penglab. janelia.org/proj/v3d). Apart from those two examples, many other visualization solutions, commercial and noncommercial, have been developed and recently surveyed (Walter *et al*., 2010).

Finally, it is worth to note that the software package Matlab (The Mathworks Inc.) has a wide user base in the image processing community in general, and many techniques presented above can be found implemented in the Matlab programming language. We also point the interested reader to a more in-depth excursion into the concepts presented above through the excellent text by Gonzalez *et al*. (2009).

Mathematical Modeling of Developmental Processes

Since the early reaction-diffusion models for morphogenesis in plants and animals (Turing, 1952; Winfree, 1972), the amount of quantitative data has grown substantially, and mathematical and physical modeling of morphogenesis has become recognized as an essential tool in developmental biology (Tomlin and Axelrod, 2007). Models are now testable and experiments motivated by them provide increased insight into how developmental processes work. This is a powerful way to convert quantitative data into useful knowledge.

Especially microscopy data can significantly increase our understanding of development, since we can directly compare model predictions with phenotypes (or more often with the results of analyzing images of phenotypes). Several recent works have formulated hypotheses about mechanisms of tissue morphogenesis in mathematical terms, based on observations from microscopy images, and coupled theoretical simulations with perturbation of experimental systems.

Drosophila has received particular attention as a model organism in combined theoretical and experimental investigations of development (Bittig *et al*., 2008; Day and Lawrence, 2000; Hufnagel *et al*., 2007; Shraiman, 2005; Solon *et al*., 2009). One of the central questions is: How does a tissue control its growth? Day and Lawrence (2000) review extracellular and intracellular regulators that link cell growth, division and cell survival to final organ size in the context of the *Drosophila* wing. They furthermore discuss models related to the hypothesis that local steepness of morphogen gradients may determine tissue size. Shraiman (2005) proposed that the mechanism for stabilizing growth may be mechanical. He uses a mathematical model for nonuniform growth and finds that cells growing faster or slower than the surrounding tissue are subject to mechanical stress, which may by itself provide a mechanism for stabilizing tissue size. Hufnagel *et al*. (2007) extend this idea. In their model the size of the wing disk is regulated by "the distance at which the morphogen signal crosses a minimum threshold necessary to promote growth." The long-range interaction necessary to propagate the information about the size of the disk is provided mechanically by stress and deformation in the growing tissue. Therefore, they formulate the coupled "proportion checkpoint" and "mechanical compression" models for wing size control.

In a closely related idea, Bittig *et al*. (2008) investigated the mechanics of tissue growth with anisotropic division and apoptosis of cells. They applied a two-dimensional coarse-grained physical description of cell movement taking into account tissue viscosity and physical parameters relevant to the *Drosophila* imaginal disk. They show that oriented cell division can control shape changes during development solely by the mechanics of the tissue through shearing. Both continuum and discrete models were implemented.

Other aspects of *Drosophila* morphogenesis observed by microscopy have also recently received attention. Farhadifar *et al*. (2007) describe a quantitative model for the *Drosophila* wing epithelial packing. In their two-dimensional discrete model, they minimize an energy functional that includes surface area constraints, line tension and possible cortical forces acting at the cell perimeter. They are able to account quantitatively for observed packing geometries and also for perturbations induced by laser ablation experiments. Solon *et al*. (Solon *et al*., 2009) focus on *Drosophila* dorsal closure. They quantitatively describe the mechanism for closure

as a cooperative force generation, in which directed tissue movement is achieved through a ratchet-like mechanism. They use a powerful combination of cell-level modeling (simulating the viscoelastic properties) and experimental perturbation of the system. Their work is an excellent example of proceeding from experiment to image analysis and then hypothesis testing in developmental biology (see Fig. 7).

CONCLUSIONS

The quantitative systems-level investigation of development with novel imaging and image processing technologies has only just begun. The future success of such studies will depend critically on combining the technological and conceptual advances in different scientific disciplines and—even more importantly—on conceiving new, sophisticated strategies to computer-aided data mining. Studying the developmental dynamics of biological systems in their entirety is a critical next step towards a comprehensive model of development and will likely be of key importance for attaining a global understanding of this multifaceted process. However, the enormous complexity intrinsic to the resulting data sets effectively precludes manual evaluation and often even detailed inspection of the experimental output. Currently, manual analyses still provide the highest level of quality control, but they also compromise the unique potential of this new experimental approach due to their low-throughput character. Effectively, there is no alternative to devising and implementing automated in silico analyses that combine human-level precision with machine-level speed to unlock truly quantitative system-level studies in microscopy-based investigations of development.

Although this goal still resides in the (hopefully not so distant) future, it is equally important to note that even this level of technical sophistication will only be a starting point. On the one hand, the powerful technologies and resources that are becoming available will enable efficient testing of a wide spectrum of hypotheses related to specific developmental and biophysical mechanisms. On the other hand, they present a great opportunity to address entirely complementary system-level questions. The developmental blueprints of a large set of individuals can be registered and compared quantitatively. Thereby, it will be possible to computationally search for recurring motifs in the spatiotemporal patterns of cell behavior underlying specific dynamic processes or even the formation of entire organs and tissues. Large-scale analyses will reveal the intrinsic variability of developmental mechanisms within single species or even individual strains as well as their conservation across species boundaries, and allow tying these quantitative insights to the respective evolutionary history. Cross-correlation of single-cell resolution morphological reconstructions and gene expression data from entire developing animals may allow systematic quantitative mapping of the genetic regulation of developmental building plans and at the same time unravel complementary mechanisms resulting e.g. from the physical forces acting during morphogenesis (Oates *et al*., 2009). The opportunities are almost endless and only one thing seems certain: These are exciting times for the emerging field of Quantitative Developmental Biology.

ACKNOWLEDGMENTS

The authors thank the authors of McMahon *et al*. 2008, Fowlkes *et al*. 2008, Fernandez *et al*. 2010, and Long *et al*. 2009 for kindly sharing their figure materials and permitting us to reprint their figures in this review article.

LITERATURE CITED

Adams R, Bischof L. 1994. Seeded region growing. IEEE Trans Pattern Anal Mach Intell 16:641–647.

Al-Kofahi KA, Lasek S, Szarowski DH, Pace CJ, Nagy G, Turner JN, Roysam B. 2002. Rapid automated three-dimensional tracing of neurons from confocal image stacks. IEEE Trans Inf Technol Biomed 6:171–187.

Al-Kofahi O, Radke RJ, Goderie SK, Shen Q, Temple S, Roysam B. 2006. Automated cell lineage construction: A rapid method to analyze clonal development established with murine neural progenitor cells. Cell Cycle 5:327–335.

Alirezaie J, Jerningan M, Nahmias C. 1997. Neural network-based segmentation of magnetic resonance images of the brain. IEEE Trans Nuclear Sci 44:194–198.

Baggett D, Nakaya MA, McAuliffe M, Yamaguchi TP, Lockett S. 2005. Whole cell segmentation in solid tissue sections. Cytometry A 67:137–143.

Bao ZR, Murray JI, Boyle T, Ooi SL, Sandel MJ, Waterston RH. 2006. Automated cell lineage tracing in *Caenorhabditis elegans*. Proc Natl Acad Sci USA 103:2707–2712.

Bittig T, Wartlick O, Kicheva A, Gonzalez-Gaitan M, Julicher F. 2008. Dynamics of anisotropic tissue growth. New J Phys 10:063001.

Bleau A, Leon LJ. 2000. Watershed-based segmentation and region merging. Comput Vis Image Und 77:317–370.

Brechbühler C, Gerig G, Kuebler O. 1995. Parametrization of closed surfaces for 3-D shape description. Comput Vision Image Und 61:154–170.

Brown KE, Keller PJ, Ramialison M, Rembold M, Stelzer EH, Loosli F, Wittbrodt J. 2010. Nlcam modulates midline convergence during anterior neural plate morphogenesis. Dev Biol 339:14–25.

Brown LG. 1992. A survey of image registration techniques. ACM Comput Surv 24:325–376.

Buytaert JA, Dirckx JJ. 2007. Design and quantitative resolution measurements of an optical virtual

sectioning three-dimensional imaging technique for biomedical specimens, featuring two-micrometer slicing resolution. J Biomed Opt 12:014039.

Campana M, Maury B, Dutreix M, Peyrieras N, Sarti A. 2010. Methods toward in vivo measurement of zebrafish epithelial and deep cell proliferation. Comput Methods Programs Biomed 98:103–117.

Campana M, Sarti A. 2010. Cell morphodynamics visualization from images of zebrafish embryogenesis. Comput Med Imaging Graph 34:394–403.

Canny J. 1986. A computational approach to edge detection. IEEE Trans Pattern Anal Machine Intelligence 8:679–714.

Caselles V, Kimmel R, Sapiro G. 1997. Geodesic active contours. Int J Comput Vis 22:61–79.

Chan TF, Vese LA. 2001. Active contours without edges. IEEE Trans Image Process 10:266–277.

Chang H, Yang Q, Parvin B. 2007. Segmentation of heterogeneous blob objects through voting and level set formulation. Pattern Recogn Lett 28: 1781–1787.

Chen SY, Hsieh CS, Chu SW, Lin CY, Ko CY, Chen YC, Tsai HJ, Hu CH, Sun CK. 2006. Noninvasive harmonics optical microscopy for long-term observation of embryonic nervous system development in vivo. J Biomed Opt 11:054022.

Chu SW, Chen SY, Tsai TH, Liu TM, Lin CY, Tsai HJ, Sun CK. 2003. In vivo developmental biology study using noninvasive multi-harmonic generation microscopy. Opt Express 11:3093–3099.

Chuai M, Dormann D, Weijer CJ. 2009. Imaging cell signalling and movement in development. Semin Cell Dev Biol 20:947–955.

Chuai M, Weijer CJ. 2009. Regulation of cell migration during chick gastrulation. Curr Opin Genet Dev 19:343–349.

Chui H, Rangarajan A. 2003. A new point matching algorithm for non-rigid registration. Comput Vis Image Und 89:114–141.

Cohen LD. 1991. On active contour models and balloons. CVGIP: Image Underst 53:211–218.

Cootes T, Taylor C, Cooper D, Graham J. 1995. Active shape models—Their training and application. Comput Vis Image Und 61:38–59.

Cui J, Acton ST, Lin Z. 2006. A Monte Carlo approach to rolling leukocyte tracking in vivo. Med Image Anal 10:598–610.

Day SJ, Lawrence PA. 2000. Measuring dimensions: The regulation of size and shape. Development 127: 2977–2987.

Debeir O, Camby I, Kiss R, Van Ham P, Decaestecker C. 2004. A model-based approach for automated in vitro cell tracking and chemotaxis analyses. Cytometry A 60:29–40.

Degerman J, Thorlin T, Faijerson J, Althoff K, Eriksson PS, Put RV, Gustavsson T. 2009. An automatic system for in vitro cell migration studies. J Microsc 233:178–191.

Denk W, Strickler JH, Webb WW. 1990. Two-photon laser scanning fluorescence microscopy. Science 248:73–76.

Diaspro A, Chirico G, Collini M. 2005. Two-photon fluorescence excitation and related techniques in biological microscopy. Q Rev Biophys 38:97–166.

Dodt HU, Leischner U, Schierloh A, Jahrling N, Mauch CP, Deininger K, Deussing JM, Eder M, Zieglgansberger W, Becker K. 2007. Ultramicroscopy: Three-dimensional visualization of neuronal networks in the whole mouse brain. Nat Methods 4:331–336.

Dormann D, Libotte T, Weijer CJ, Bretschneider T. 2002. Simultaneous quantification of cell motility and protein-membrane-association using active contours. Cell Motil Cytoskeleton 52:221–230.

Duda R, Hart P. 1973. Pattern classification and scene analysis. New York: Wiley.

Dufour A, Shinin V, Tajbakhsh S, Guillen-Aghion N, Olivo-Marin JC, Zimmer C. 2005. Segmenting and tracking fluorescent cells in dynamic 3-D microscopy with coupled active surfaces. IEEE Trans Image Process 14:1396–1410.

Engelbrecht CJ, Greger K, Reynaud EG, Krzic U, Colombelli J, Stelzer EH. 2007. Three-dimensional laser microsurgery in light-sheet based microscopy (SPIM). Opt Express 15:6420–6430.

England SJ, Adams RJ. 2007. Building a dynamic fate map. Biotechniques 43:20–24.

England SJ, Blanchard GB, Mahadevan L, Adams RJ. 2006. A dynamic fate map of the forebrain shows how vertebrate eyes form and explains two causes of cyclopia. Development 133:4613–4617.

Ezin AM, Fraser SE, Bronner-Fraser M. 2009. Fate map and morphogenesis of presumptive neural crest and dorsal neural tube. Dev Biol 330:221–236.

Farhadifar R, Roper JC, Aigouy B, Eaton S, Julicher F. 2007. The influence of cell mechanics, cell-cell interactions, and proliferation on epithelial packing. Curr Biol 17:2095–2104.

Fernandez R, Das P, Mirabet V, Moscardi E, Traas J, Verdeil JL, Malandain G, Godin C. 2010. Imaging plant growth in 4D: robust tissue reconstruction and lineaging at cell resolution. Nat Methods 7:547–553.

Fowlkes CC, Hendriks CL, Keranen SV, Weber GH, Rubel O, Huang MY, Chatoor S, DePace AH, Simirenko L, Henriquez C, Beaton A, Weiszmann R, Celniker S, Hamann B, Knowles DW, Biggin MD, Eisen MB, Malik J. 2008. A quantitative spatiotemporal atlas of gene expression in the Drosophila blastoderm. Cell 133:364–374.

Frise E, Hammonds AS, Celniker SE. 2010. Systematic image-driven analysis of the spatial Drosophila embryonic expression landscape. Mol Syst Biol 6:345.

Fuchs E, Jaffe J, Long R, Azam F. 2002. Thin laser light sheet microscope for microbial oceanography. Opt Express 10:145–154.

Gold S, Rangarajan A. 1996. A graduated assignment algorithm for graph matching. IEEE Trans Pattern Anal Machine Intell 18:377–388.

Gong Y, Mo C, Fraser SE. 2004. Planar cell polarity signalling controls cell division orientation during zebrafish gastrulation. Nature 430:689–693.

Gonzalez R, Woods R, Eddins S. 2009. Digital image processing using Matlab, 2nd edition, Gatesmark Publishing.

Gor V, Elowitz M, Bacarian T, Mjolsness E. 2005.Tracking cell signals in fluorescent images. Proceedings of the IEEE Computer Society Conference on Computer Vision and Pattern Recognition, CVPR 2005, Los Alamitos, CA.

Graf R, Rietdorf J, Zimmermann T. 2005. Live cell spinning disk microscopy. Adv Biochem Eng Biotechnol 95:57–75.

Hadjantonakis AK, Dickinson ME, Fraser SE, Papaioannou VE. 2003. Technicolour transgenics: Imaging tools for functional genomics in the mouse. Nat Rev Genet 4:613–625.

Hadjantonakis AK, Papaioannou VE. 2004. Dynamic in vivo imaging and cell tracking using a histone fluorescent protein fusion in mice. BMC Biotechnol 4:33.

Heid PJ, Voss E, Soll DR. 2002. 3D-DIASemb: A computer-assisted system for reconstructing and motion analyzing in 4D every cell and nucleus in a developing embryo. Dev Biol 245:329–347.

Held M, Schmitz MH, Fischer B, Walter T, Neumann B, Olma MH, Peter M, Ellenberg J, Gerlich DW. 2010. CellCognition: Time-resolved phenotype annotation in high-throughput live cell imaging. Nat Methods 7:747–754.

Helmchen F, Denk W. 2005. Deep tissue two-photon microscopy. Nat Methods 2:932–940.

Hirose Y, Varga ZM, Kondoh H, Furutani-Seiki M. 2004. Single cell lineage and regionalization of cell populations during Medaka neurulation. Development 131:2553–2563.

Holekamp TF, Turaga D, Holy TE. 2008. Fast three-dimensional fluorescence imaging of activity in neural populations by objective-coupled planar illumination microscopy. Neuron 57:661–672.

Hom EFY, Marchis F, Lee TK, Haase S, Agard DA, Sedat JW. 2007. AIDA: An adaptive image deconvolution algorithm with application to multi-frame and three-dimensional data. J Opt Soc Am A 24:1580–1600.

Hsieh CS, Ko CY, Chen SY, Liu TM, Wu JS, Hu CH, Sun CK. 2008. In vivo long-term continuous observation of gene expression in zebrafish embryo nerve systems by using harmonic generation microscopy and morphant technology. J Biomed Opt 13:064041.

Huang D, Swanson EA, Lin CP, Schuman JS, Stinson WG, Chang W, Hee MR, Flotte T, Gregory K, Puliafito CA, *et al*. 1991. Optical coherence tomography. Science 254:1178–1181.

Hufnagel L, Teleman AA, Rouault H, Cohen SM, Shraiman BI. 2007. On the mechanism of wing size determination in fly development. Proc Natl Acad Sci USA 104:3835–3840.

Huisken J, Stainier DY. 2007. Even fluorescence excitation by multidirectional selective plane illumination microscopy (mSPIM). Opt Lett 32:2608–2610.

Huisken J, Stainier DY. 2009. Selective plane illumination microscopy techniques in developmental biology. Development 136:1963–1975.

Huisken J, Swoger J, Del Bene F, Wittbrodt J, Stelzer EH. 2004. Optical sectioning deep inside live embryos by selective plane illumination microscopy. Science 305:1007–1009.

Jacobs RE, Papan C, Ruffins S, Tyszka JM, Fraser SE. 2003. MRI: Volumetric imaging for vital imaging and atlas construction. Nat Rev Mol Cell Biol 4:S10–S16.

Jaqaman K, Loerke D, Mettlen M, Kuwata H, Grinstein S, Schmid SL, Danuser G. 2008. Robust single-particle tracking in live-cell time-lapse sequences. Nat Methods 5:695–702.

Kachouie N, Fieguth P, Ramunas J, Jervis E. 2006. Probabilistic model-based cell tracking. Int J Biomed Imaging 2006:12186.

Kass M, Witkin A, Terzopoulos D. 1988. Snakes: Active contour models. Int J Comput Vis 1:321–331.

Keller PJ, Pampaloni F, Lattanzi G, Stelzer EH. 2008a. Three-dimensional microtubule behavior in Xenopus egg extracts reveals four dynamic states and state-dependent elastic properties. Biophys J 95:1474–1486.

Keller PJ, Pampaloni F, Stelzer EH. 2006. Life sciences require the third dimension. Curr Opin Cell Biol 18:117–124.

Keller PJ, Pampaloni F, Stelzer EH. 2007. Three-dimensional preparation and imaging reveal intrinsic microtubule properties. Nat Methods 4:843–846.

Keller PJ, Schmidt AD, Santella A, Khairy K, Bao Z, Wittbrodt J, Stelzer EH. 2010. Fast, high-contrast imaging of animal development with scanned light sheet-based structured-illumination microscopy. Nat Methods 7:637–642.

Keller PJ, Schmidt AD, Wittbrodt J, Stelzer EH. 2008b. Reconstruction of zebrafish early embryonic development by scanned light sheet microscopy. Science 322:1065–1069.

Keller PJ, Stelzer EH. 2008. Quantitative in vivo imaging of entire embryos with digital scanned laser light sheet fluorescence microscopy. Curr Opin Neurobiol 18:624–632.

Keller PJ, Stelzer EH. 2010. Digital scanned laser light sheet fluorescence microscopy. Cold Spring Harb Protoc 2010:pdb top78.

Keranen SV, Fowlkes CC, Luengo Hendriks CL, Sudar D, Knowles DW, Malik J, Biggin MD. 2006. Three-

dimensional morphology and gene expression in the Drosophila blastoderm at cellular resolution II: dynamics. Genome Biol 7:R124.

Khairy K, Foo J, Howard J. 2008a. Shapes of red blood cells: Comparison of 3D confocal images with the bilayer-couple model. Cell Mol Bioeng 1:173–181.

Khairy K, Howard J. 2008. Spherical harmonics-based parametric deconvolution of 3D surface images using bending energy minimization. Med Image Anal 12:217–227.

Khairy K, Reynaud E, Stelzer E. 2008b. Detection of deformable objects in 3D images using Markov-Chain Monte Carlo and spherical harmonics. Med Image Comput Comput Assist Interv 11: 1075–1082.

Koster RW, Fraser SE. 2004. Time-lapse microscopy of brain development. Methods Cell Biol 76:207–235.

Krieg M, Arboleda-Estudillo Y, Puech PH, Kafer J, Graner F, Muller DJ, Heisenberg CP. 2008. Tensile forces govern germ-layer organization in zebrafish. Nat Cell Biol 10:429–436.

Kriva Z, Mikula K, Peyrieras N, Rizzi B, Sarti A, Stasova O. 2010. 3D early embryogenesis image filtering by nonlinear partial differential equations. Med Image Anal 14:510–526.

Kulesa PM, Bailey CM, Cooper C, Fraser SE. 2010. In ovo live imaging of avian embryos. Cold Spring Harb Protoc 2010:pdb prot5446.

Kulesa PM, Fraser SE. 2002. Cell dynamics during somite boundary formation revealed by time-lapse analysis. Science 298:991–995.

Lam EY, Goodman JW. 2000. Iterative statistical approach to blind image deconvolution. J Opt Soc Am A Opt Image Sci Vis 17:1177–1184.

Larin KV, Larina IV, Liebling M, Dickinson ME. 2009. Live imaging of early developmental processes in mammalian embryos with optical coherence tomography. J Innov Opt Health Sci 2:253–259.

Li G, Liu T, Nie J, Guo L, Chen J, Zhu J, Xia W, Mara A, Holley S, Wong ST. 2008a. Segmentation of touching cell nuclei using gradient flow tracking. J Microsc 231:47–58.

Li G, Liu T, Nie J, Guo L, Malicki J, Mara A, Holley SA, Xia W, Wong ST. 2007a. Detection of blob objects in microscopic zebrafish images based on gradient vector diffusion. Cytometry A 71:835–845.

Li G, Liu T, Tarokh A, Nie J, Guo L, Mara A, Holley S, Wong ST. 2007b. 3D cell nuclei segmentation based on gradient flow tracking. BMC Cell Biol 8:40.

Li K, Miller ED, Chen M, Kanade T, Weiss LE, Campbell PG. 2008b. Cell population tracking and lineage construction with spatiotemporal context. Med Image Anal 12:546–566.

Li S. 1995. Markov random field modeling in computer vision. Tokyo: Springer.

Liebling M, Forouhar AS, Wolleschensky R, Zimmermann B, Ankerhold R, Fraser SE, Gharib M, Dickinson ME. 2006. Rapid three-dimensional imaging and analysis of the beating embryonic heart reveals functional changes during development. Dev Dyn 235:2940–2948.

Liu M, Roy-Chowdhury AK, Gonehal VR. 2009a.Exploiting local structure for tracking plant cells in noisy images. Proceedings of the International Conference on Image Processing, ICIP 2009, Cairo, Egypt.

Liu T, Li G, Nie J, Tarokh A, Zhou X, Guo L, Malicki J, Xia W, Wong ST. 2008. An automated method for cell detection in zebrafish. Neuroinformatics 6:5–21.

Liu X, Long FH, Peng HC, Aerni SJ, Jiang M, Sanchez-Blanco A, Murray JI, Preston E, Mericle B, Batzoglou S, Myers EW, Kim SK. 2009b. Analysis of cell fate from single-cell gene expression profiles in *C. elegans*. Cell 139:623–633.

Long FH, Peng HC, Liu X, Kim SK, Myers E. 2009. A 3D digital atlas of *C. elegans* and its application to single-cell analyses. Nat Methods 6:667–672.

Lucy LB. 1974. An iterative technique for the rectification of observed distributions. Astronomical J 79:745–754.

Luengo Hendriks CL, Keranen SV, Biggin MD, Knowles DW. 2007. Automatic channel unmixing for high-throughput quantitative analysis of fluorescence images. Opt Express 15:12306–12317.

Luengo Hendriks CL, Keranen SV, Fowlkes CC, Simirenko L, Weber GH, DePace AH, Henriquez C, Kaszuba DW, Hamann B, Eisen MB, Malik J, Sudar D, Biggin MD, Knowles DW. 2006. Three-dimensional morphology and gene expression in the Drosophila blastoderm at cellular resolution I: Data acquisition pipeline. Genome Biol 7:R123.

MacAulay C, Palcic B. 1988. A comparison of some quick and simple threshold selection methods for stained cells. Anal Quant Cytol Histol 10:134–138.

Mace DL, Lee JY, Twigg RW, Colinas J, Benfey PN, Ohler U. 2006. Quantification of transcription factor expression from Arabidopsis images. Bioinformatics 22:e323–331.

Markham J, Conchello JA. 1999. Parametric blind deconvolution: A robust method for the simultaneous estimation of image and blur. J Opt Soc Am A Opt Image Sci Vis 16:2377–2391.

Marr D, Hildreth E. 1980. Theory of edge detection. Proc R Soc Lond B Biol Sci 207:187–217.

Martinelli SD, Brown CG, Durbin R. 1997. Gene expression and development databases for *C. elegans*. Semin Cell Dev Biol 8:459–467.

Mavrakis M, Pourquie O, Lecuit T. 2010. Lighting up developmental mechanisms: How fluorescence imaging heralded a new era. Development 137:373–387.

Mavrakis M, Rikhy R, Lilly M, Lippincott-Schwartz J. 2008. Fluorescence imaging techniques for studying Drosophila embryo development. Curr Protoc Cell Biol Chapter 4:Unit 4.18.

McInerney T, Terzopoulos D. 1995. A dynamic finite element surface model for segmentation and tracking in multidimensional medical images with application to cardiac 4D image analysis. Comput Med Imaging Graph 19:69–83.

McInerney T, Terzopoulos D. 1996. Deformable models in medical image analysis: A survey. Med Image Anal 1:91–108.

McMahon A, Supatto W, Fraser SE, Stathopoulos A. 2008. Dynamic analyses of Drosophila gastrulation provide insights into collective cell migration. Science 322:1546–1550.

Megason SG, Fraser SE. 2003. Digitizing life at the level of the cell: high-performance laser-scanning microscopy and image analysis for in toto imaging of development. Mech Dev 120:1407–1420.

Megason SG, Fraser SE. 2007. Imaging in systems biology. Cell 130:784–795.

Melani C, Campana M, Lombardot B, Rizzi B, Veronesi F, Zanella C, Bourgine P, Mikula K, Peyrieras N, Sarti A. 2007. Cells tracking in a live zebrafish embryo. Conf Proc IEEE Eng Med Biol Soc 2007:1631–1634.

Mertz J, Kim J. 2010. Scanning light-sheet microscopy in the whole mouse brain with HiLo background rejection. J Biomed Opt 15:016027.

Modayur B, Prothero J, Ojemann G, Maravilla K, Brinkley J. 1997. Visualization-based mapping of language function in the brain. NeuroImage 6:245–258.

Mohamed N, Ahmed M, Farag A. 1999.Modified Fuzzy C-mean in medical image segmentation. In: IEEE International Conference on Acoustics, Speech, and Signal Processing Phoenix, AZ.

Moore P, Molloy D. 2007.A survey of computer-based deformable models. International Machine Vision and Image Processing Conference, IMVIP 2007, Maynooth, Ireland.

Mukherjee DP, Ray N, Acton ST. 2004. Level set analysis for leukocyte detection and tracking. IEEE Trans Image Process 13:562–572.

Murray JI, Bao Z, Boyle TJ, Boeck ME, Mericle BL, Nicholas TJ, Zhao Z, Sandel MJ, Waterston RH. 2008. Automated analysis of embryonic gene expression with cellular resolution in C-elegans. Nat Methods 5:703–709.

Murray JI, Bao ZR, Boyle TJ, Waterston RH. 2006. The lineaging of fluorescently-labeled *Caenorhabditis elegans* embryos with StarryNite and AceTree. Nat Protocols 1:1468–1476.

Nowotschin S, Eakin GS, Hadjantonakis AK. 2009. Live-imaging fluorescent proteins in mouse embryos: Multi-dimensional, multi-spectral perspectives. Trends Biotechnol 27:266–276.

Nowotschin S, Hadjantonakis AK. 2009a. Photomodulatable fluorescent proteins for imaging cell dynamics and cell fate. Organogenesis 5:135–144.

Nowotschin S, Hadjantonakis AK. 2009b. Use of KikGR a photoconvertible green-to-red fluorescent protein for cell labeling and lineage analysis in ES cells and mouse embryos. BMC Dev Biol 9:49.

Nowotschin S, Ferrer-Vaquer A, Hadjantonakis AK. 2010. Imaging mouse development with confocal time-lapse microscopy. Methods Enzymol 476:351–377.

Nowotschin S, Hadjantonakis AK. 2010. Cellular dynamics in the early mouse embryo: From axis formation to gastrulation. Curr Opin Genet Dev 20:420–427.

Oates AC, Gorfinkiel N, Gonzalez-Gaitan M, Heisenberg CP. 2009. Quantitative approaches in developmental biology. Nat Rev Genet 10:517–530.

Olivier N, Luengo-Oroz MA, Duloquin L, Faure E, Savy T, Veilleux I, Solinas X, Debarre D, Bourgine P, Santos A, Peyrieras N, Beaurepaire E. 2010. Cell lineage reconstruction of early zebrafish embryos using label-free nonlinear microscopy. Science 329:967–971.

Osher S, Sethian JA. 1988. Fronts propagating with curvature-dependent speed: Algorithms based on Hamilton-Jacobi formulations. J Comput Phys 79:12–49.

Otsu N. 1979. A threshold selection method from gray-level histograms. IEEE Trans Syst Man Cubern 9:62–66.

Padfield D, Rittscher J, Roysam B. 2009a. Coupled minimum-cost flow cell tracking. Inf Process Med Imaging 21:374–385.

Padfield D, Rittscher J, Thomas N, Roysam B. 2009b. Spatio-temporal cell cycle phase analysis using level sets and fast marching methods. Med Image Anal 13:143–155.

Palero J, Santos SI, Artigas D, Loza-Alvarez P. 2010. A simple scanless two-photon fluorescence microscope using selective plane illumination. Opt Express 18:8491–8498.

Paluch E, Heisenberg CP. 2009. Biology and physics of cell shape changes in development. Curr Biol 19:R790–R799.

Pampaloni F, Reynaud EG, Stelzer EH. 2007. The third dimension bridges the gap between cell culture and live tissue. Nat Rev Mol Cell Biol 8:839–845.

Papan C, Boulat B, Velan SS, Fraser SE, Jacobs RE. 2007. Formation of the dorsal marginal zone in *Xenopus laevis* analyzed by time-lapse microscopic magnetic resonance imaging. Dev Biol 305:161–171.

Parton RM, Valles AM, Dobbie IM, Davis I. 2010. Live cell imaging in Drosophila melanogaster. Cold Spring Harb Protoc 2010:pdb top75.

Pavlidis T. 1992. Why progress in machine vision is so slow. Pattern Recogn Lett 13:221–225.

Pawley J. 2006. Handbook of biological confocal microscopy: New York: Springer.

Pecreaux J, Zimmer C, Olivo-Marin J. 2006. Biophysical active contours for cell tracking. I. Tension and bending. In: ICIP 2006. Atlanta, USA.

Peng H, Long F, Zhou J, Leung G, Eisen MB, Myers EW. 2007. Automatic image analysis for gene expression patterns of fly embryos. BMC Cell Biol 8:S7.

Peng HC, Long FH, Liu X, Kim SK, Myers EW. 2008. Straightening *Caenorhabditis elegans* images. Bioinformatics 24:234–242.

Peng HC, Long FH, Myers EW. 2009. VANO: A volume-object image annotation system. Bioinformatics 25:695–697.

Peng HC, Ruan ZC, Long FH, Simpson JH, Myers EW. 2010. V3D enables real-time 3D visualization and quantitative analysis of large-scale biological image data sets. Nat Biotechnol 28:348–353.

Perona P, Malik J. 1990. Scale-space and edge detection using anisotripic diffusion. IEEE Trans Pattern Anal Machine Intell 12:629–639.

Preibisch S, Saalfeld S, Schindelin J, Tomancak P. 2010. Software for bead-based registration of selective plane illumination microscopy data. Nat Methods 7:418–419.

Rabut G, Ellenberg J. 2004. Automatic real-time three-dimensional cell tracking by fluorescence microscopy. J Microsc 216:131–137.

Racine V, Sachse M, Salamero J, Fraisier V, Trubuil A, Sibarita JB. 2007. Visualization and quantification of vesicle trafficking on a three-dimensional cytoskeleton network in living cells. J Microsc 225:214–228.

Ray N, Acton ST, Ley K. 2002. Tracking leukocytes in vivo with shape and size constrained active contours. IEEE Trans Med Imaging 21:1222–1235.

Rembold M, Loosli F, Adams RJ, Wittbrodt J. 2006. Individual cell migration serves as the driving force for optic vesicle evagination. Science 313:1130–1134.

Revol-Muller C, Peyrin F, Carrillon Y, Odet C. 2002. Automated 3D region growing algorithm based on an assessment function. Pattern Recogn Lett 23:137–150.

Revol C, Jourlin M. 1997. A new minimum variance region growing algorithm for image segmentation. Pattern Recogn Lett 18:249–258.

Rhee JM, Oda-Ishii I, Passamaneck YJ, Hadjantonakis AK, Di Gregorio A. 2005. Live imaging and morphometric analysis of embryonic development in the ascidian Ciona intestinalis. Genesis 43:136–147.

Rizzi B, Campana M, Zanella C, Melani C, Cunderlik R, Kriva Z, Bourgine P, Mikula K, Peyrieras N, Sarti A. 2007. 3-D zebrafish embryo image filtering by nonlinear partial differential equations. Conf Proc IEEE Eng Med Biol Soc 2007:6252–6255.

Rizzi B, Sarti A. 2009. Region-based PDEs for cells counting and segmentation in 3D+time images of vertebrate early embryogenesis. Int J Biomed Imaging 2009:968986.

Roerdink JBTM, Meijster A. 2001. The watershed transform: Definitions, algorithms and parallelization strategies. Fundamenta Informaticae 21:187–228.

Rohrbach A. 2009. Artifacts resulting from imaging in scattering media: A theoretical prediction. Opt Lett 34:3041–3043.

Rose K. 1998. Deterministic annealing for clustering, compression, classification, regression, and related optimization problems. Proceedings of the IEEE 86:2210–2239.

Ruffins SW, Martin M, Keough L, Truong S, Fraser SE, Jacobs RE, Lansford R. 2007. Digital three-dimensional atlas of quail development using high-resolution MRI. Scientific World J 7:592–604.

Russel R, Adams N, Stephens D, Batty E, Jensen K. 2009. Segmentation of fluorescence microscopy images for quantitative analysis of cell nuclear architecture. Biophys J 96:3379–3389.

Sarti A, Malladi R, Sethian JA. 2000. Subjective surfaces: A method for completing missing boundaries. Proc Natl Acad Sci USA 97:6258–6263.

Scherz PJ, Huisken J, Sahai-Hernandez P, Stainier DY. 2008. High-speed imaging of developing heart valves reveals interplay of morphogenesis and function. Development 135:1179–1187.

Schnabel R, Hutter H, Moerman D, Schnabel H. 1997. Assessing normal embryogenesis in *Caenorhabditis elegans* using a 4D microscope: Variability of development and regional specification. Dev Biol 184: 234–265.

Serra J. 1982. Image analysis and mathematical morphology. San Diego: Academic Press.

Sharpe J, Ahlgren U, Perry P, Hill B, Ross A, Hecksher-Sorensen J, Baldock R, Davidson D. 2002. Optical projection tomography as a tool for 3D microscopy and gene expression studies. Science 296:541–545.

Shen HL, Nelson G, Kennedy S, Nelson D, Johnson J, Spiller D, White MRH, Kell DB. 2006. Automatic tracking of biological cells and compartments using particle filters and active contours. Chemometrics Intelligent Lab Syst 82:276–282.

Shraiman BI. 2005. Mechanical feedback as a possible regulator of tissue growth. Proc Natl Acad Sci USA 102:3318–3323.

Siedentopf H, Zsigmondy R. 1903. Über Sichtbarmachung und Größenbestimmung ultramikroskopischer Teilchen, mit besonderer Anwendung auf Goldrubingläser. Ann Phys 315:1–39.

Solon J, Kaya-Copur A, Colombelli J, Brunner D. 2009. Pulsed forces timed by a ratchet-like mechanism drive directed tissue movement during dorsal closure. Cell 137:1331–1342.

Sonka M, Hlavac V, Boyle R. 1998.Image Processing: Analysis and Machine Vision: CL-Engineering.

Spalteholz W. 1914. Über das Durchsichtigmachen von menschlichen und tierischen Präparaten. Leipzig: S. Hirzel.

Stelzer EHK, Lindek S. 1994. Fundamental reduction of the observation volume in far-field light microscopy by detection orthogonal to the illumination axis: confocal theta microscopy. Opt Comm 111:536–547.

Styner M, Lieberman JA, McClure RK, Weinberger DR, Jones DW, Gerig G. 2005. Morphometric analysis of lateral ventricles in schizophrenia and healthy controls regarding genetic and disease-specific factors. Proc Natl Acad Sci USA 102:4872–4877.

Sun CK, Chu SW, Chen SY, Tsai TH, Liu TM, Lin CY, Tsai HJ. 2004. Higher harmonic generation microscopy for developmental biology. J Struct Biol 147:19–30.

Sun Y. 1989. Automated identification of vessel contours in coronary arteriograms by an adaptive tracking algorithm. IEEE Trans Med Imaging 8:78–88.

Supatto W, McMahon A, Fraser SE, Stathopoulos A. 2009. Quantitative imaging of collective cell migration during Drosophila gastrulation: Multiphoton microscopy and computational analysis. Nat Protoc 4:1397–1412.

Swoger J, Verveer P, Greger K, Huisken J, Stelzer EH. 2007. Multi-view image fusion improves resolution in three-dimensional microscopy. Opt Express 15:8029–8042.

Szekely G, Gerig G. 2000. Model-based segmentation of radiological images. Kuenstliche Intelligenz 3:18–23.

Tassy O, Daian F, Hudson C, Bertrand V, Lemaire P. 2006. A quantitative approach to the study of cell shapes and interactions during early chordate embryogenesis. Curr Biol 16:345–358.

Terzopoulos D, McInerney T. 1997. Deformable models and the analysis of medical images. Stud Health Technol Inform 39:369–378.

Tobias OJ, Seara R. 2002. Image segmentation by histogram thresholding using fuzzy sets. IEEE Trans Image Process 11:1457–1465.

Tomer R, Denes AS, Tessmar-Raible K, Arendt D. 2010. Profiling by image registration reveals common origin of annelid mushroom bodies and vertebrate pallium. Cell 142:800–809.

Tomlin CJ, Axelrod JD. 2007. Biology by numbers: Mathematical modelling in developmental biology. Nat Rev Genet 8:331–340.

Turaga D, Holy TE. 2008. Miniaturization and defocus correction for objective-coupled planar illumination microscopy. Opt Lett 33:2302–2304.

Turing AM. 1952. The chemical basis of morphogenesis. Philos Trans Roy Soc Lond Series B, Biol Sci 237: 37–72.

Udan RS, Dickinson ME. 2010. Imaging mouse embryonic development. Methods Enzymol 476:329–349.

Verveer PJ, Swoger J, Pampaloni F, Greger K, Marcello M, Stelzer EH. 2007. High-resolution three-dimensional imaging of large specimens with light sheet-based microscopy. Nat Methods 4:311–313.

Vincent L, Soille P. 1991. Watersheds in digital spaces: An efficient algorithm based on immersion simulations. IEEE Trans Pattern Anal Machine Intell 13: 583–593.

Voie AH, Burns DH, Spelman FA. 1993. Orthogonal-plane fluorescence optical sectioning: Three-dimensional imaging of macroscopic biological specimens. J Microsc 170:229–236.

Walter T, Shattuck DW, Baldock R, Bastin ME, Carpenter AE, Duce S, Ellenberg J, Fraser A, Hamilton N, Pieper S, Ragan MA, Schneider JE, Tomancak P, Heriche JK. 2010. Visualization of image data from cells to organisms. Nat Methods 7:S26–S41.

Wang S, Zhu W, Liang Z-P. 2001. Shape deformation: SVM Regression and application to medical image segmentation. Eighth International Conference on Computer Vision, 2:209.

Weber GH, Rubel O, Huang MY, DePace AH, Fowlkes CC, Keranen SVE, Hendriks CLL, Hagen H, Knowles DW, Malik J, Biggin MD, Hamann B. 2009. Visual exploration of three-dimensional gene expression using physical views and linked abstract views. IEEE-Acm Trans Comp Biol Bioinform 6:296–309.

Winfree AT. 1972. Spiral waves of chemical activity. Science 175:634–636.

Wittbrodt J, Shima A, Schartl M. 2002. Medaka—A model organism from the far East. Nat Rev Genet 3:53–64.

Xu C, Prince J. 1998. Snakes, shapes, and gradient vector flow. IEEE Trans Image Proc 7:359–369.

Yin C, Ciruna B, Solnica-Krezel L. 2009. Convergence and extension movements during vertebrate gastrulation. Curr Top Dev Biol 89:163–192.

Yu W, Lee HK, Hariharan S, Bu W, Ahmed S. 2009a. Quantitative neurite outgrowth measurement based on image segmentation with topological dependence. Cytometry A 75:289–297.

Yu W, Lee HK, Hariharan S, Bu W, Ahmed S. 2010. Evolving generalized Voronoi diagrams for accurate cellular image segmentation. Cytometry A 77:379–386.

Yu W, Lee HK, Hariharan S, Sankaran S, Vallotton P, Ahmed S. 2009b. Segmentation of neural stem/progenitor cells nuclei within 3-D neurospheres. In: Proceedings of the 5th International Symposium on Advances in Visual Computing: Part I. Las Vegas: Springer. pp 531–543.

Zamir EA, Czirok A, Rongish BJ, Little CD. 2005. A digital image-based method for computational tissue fate mapping during early avian morphogenesis. Ann Biomed Eng 33:854–865.

Zamperoni P. 1996. Plus ca va, moins ca va. Pattern Recogn Lett 17:671–677.

Zanella C, Campana M, Rizzi B, Melani C, Sanguinetti G, Bourgine P, Mikula K, Peyrieras N, Sarti A. 2010. Cells segmentation from 3-D confocal images of early zebrafish embryogenesis. IEEE Trans Image Process 19:770–781.

Zanella C, Rizzi B, Melani C, Campana M, Bourgine P, Mikula K, Peyrieras N, Sarti A. 2007. Segmentation of cells from 3-D confocal images of live zebrafish embryo. Conf Proc IEEE Eng Med Biol Soc 2007:6028–6031.

Zhou J, Peng H. 2007. Automatic recognition and annotation of gene expression patterns of fly embryos. Bioinformatics 23:589–596.

Zimmer C, Labruyere E, Meas-Yedid V, Guillen N, Olivo-Marin JC. 2002. Segmentation and tracking of migrating cells in videomicroscopy with parametric active contours: A tool for cell-based drug testing. IEEE Trans Med Imaging 21:1212–1221.

Zitova B. 2003. Image registration methods: A survey. Image Vis Comp 21:977–1000.